IAEA
International Atomic Energy Agency

INDC (NDS)-0495
Distr. A,DC,NE,SK

INDC International Nuclear Data Committee

Summary Report of
Second IAEA Research Co-ordination Meeting

Tritium Inventory in Fusion Reactors

Prepared by
R.E.H. Clark

IAEA Headquarters, Vienna, Austria
18-19 October 2004

IAEA Nuclear Data Section, Wagramer Strasse 5, A-1400 Vienna, Austria

Selected INDC documents may be downloaded in electronic form from *http://www-nds.iaea.org/indc_sel.html* or sent as an e-mail attachment. Requests for hardcopy or e-mail transmittal should be directed to *services@iaeand.iaea.org* or to:

Nuclear Data Section
International Atomic Energy Agency
PO Box 100
Wagramer Strasse 5
A-1400 Vienna
Austria

Produced by the IAEA in Austria
March 2006

INDC(NDS)-0495

Summary Report of

Second IAEA Research Co-ordination Meeting

Tritium Inventory in Fusion Reactors

Prepared by

R.E.H. Clark

IAEA Headquarters, Vienna, Austria

18-19 October 2004

Abstract

Detailed discussions were held during an RCM at IAEA Headquarters on 18-19 October 2004 to review the progress made in the CRP on "Tritium Inventory in Fusion Reactors". Participants summarized the specific results obtained during the initial phase of the Coordinated Research Project (CRP), and considered the impact of the data generated on the design of fusion devices. Areas with further research needs were identified, and a set of outstanding objectives was formulated for the continuation of the CRP. The discussions, conclusions and recommendations of the RCM are briefly described in this report.

March 2006

TABLE OF CONTENTS

1. Introduction

A second Research Coordination Meeting (RCM) dedicated to "Tritium inventory in fusion reactors" was held on 18-19 October 2004 at IAEA Headquarters, Vienna. The main purposes of this RCM were to review the research activities of the participants and identify additional data needs for tritium issues that require continued study. All eleven participants are experts in the study and understanding of the interactions of hydrogen isotopes with likely fusion reactor plasma-facing materials (Appendix 1).

2. Meeting Proceedings

A. Nichols (Section Head, Nuclear Data Section) welcomed the participants on behalf of the International Atomic Energy Agency (IAEA). He noted that there are many processes of importance in gaining a sound understand of the overall inventory of tritium in fusion machines, including deposition, retention and release mechanisms. The overall inventory of tritium in ITER will be a major issue due to strict limits on the total tritium allowed in the machine for safety reasons. He expressed optimism that the CRP will continue to provide valuable new data on these processes.

R. Clark (Scientific Secretary) reviewed the proposed agenda, which was accepted without change (Appendix 2).

2.1 Summary of current research activities

Each participant gave a detailed presentation of their research activities during the initial phase of the CRP, and provided short written summaries (Appendix 3). These presentations have been collected together electronically and distributed on CD; only brief summaries are given in this section. A work plan was also formulated for the necessary continuation of the CRP.

T. Tanabe presented recent work on the retention of hydrogen isotopes and carbon deposition. Comparisons were made among the three major fusion devices: JET, TFTR and JT-60U. The tritium deposition profiles in JET and TFTR were observed to be very consistent with the carbon deposition, and the hydrogen concentrations in both sets of deposits were homogenous. However, tritium retention on the erosion-dominated sides of the tiles was very high in TFTR, and tritium penetration into the gap indicated two different processes. On the plasma-facing surface and in the shallow gap, the carbon transport mechanism is likely to be cyclic erosion and prompt re-deposition. Tritium retention and hence carbon deposition in the gap is rather small in JET, while tritium retention in the plasma-shadowed area at the inner pumping slot is significant (unclear whether plasma processes or neutral transport dominate the carbon deposition in this particular area). Deposition on the inner divertor of JT-60U seems to be similar to JET, although no significant deposition was observed on the plasma-shadowed area or in the pumping slot (deposition profiles are toroidally more uniform). The deposited layers retain hydrogen homogeneously with depth, except for a few surface layers that are a few mm deep. Surface D within a depth of a few mm is mostly replaced by H, an indication of possible T removal by D discharges. High-energy D originating from neutral beam injection is not negligible, and has proved to be difficult to remove. Differences between JET and JT-60 may be due to divertor geometry, including magnetic field lines and divertor structure; tile shape and alignment also seem to play an important role.

S.V. Artemov reported on the NERD method for the study of concentration profiles of tritium within the interior elements of fusion reactors. NERD is a nondestructive method of determining the depth profiles of hydrogen isotopes in materials. All hydrogen isotopes are analyzed simultaneously by means of this technique, and analyses can be undertaken irrespective of the condition of the tested material (gas, liquid, or solid). The maximum depth of analysis is defined by the range of recoiled nucleus in the bulk material. Design considerations were discussed, including an assessment of the causes and mitigation of background signals, along with methods of optimizing the depth resolution. Modifications to the spectrometer were described, and included a comprehensive review of the electronics and analytical software. Laboratory tests of the procedure for determining tritium and deuterium in titanium were described, and demonstrated that significant improvements have taken place. Plans for future work include:

(a) design, manufacture and mounting of a device for the adjustable translocation of a well-focused deuteron beam on a target to check the beam location;
(b) continued development of the target unit for operation with the neutron flux at the optimal angle;
(c) improvements to the fast gates in order to decrease the effect of the driving signal on the spectrometric signal;
(d) analysis of the interfering reactions with triton escape on the nuclei of materials used in the construction of thermonuclear reactors;
(e) measurements of the content and depth profiles of hydrogen isotopes in the materials of thermonuclear reactors.

J. Roth summarized results from the depth profiling of deuterium in tungsten-based alloys that are likely to be used as the plasma-facing materials in future fusion devices such as ITER. Hydrogen depth profiles can provide detailed information on the depth distribution of defects responsible for hydrogen trapping. Hydrogen retention depends on the crystalline structure of tungsten, and therefore comparisons were made between single crystal and polycrystalline samples. Details of the experimental set-up were described, in which deuterium depth profiling was carried out using the $D(^3He, p)^4He$ nuclear reaction. The analyzing ^3He beam covered the energy range from 0.69 to 4.0 MeV, and the SIMNRA computer program was used to de-convolute the proton yield. Depth profiles of deuterium trapped in W materials were determined up to a depth of 7 μm. The depth at which deuterium is retained in W single crystals and polycrystalline W was found to be divisible into three zones:

(a) near-surface layer (up to a depth of ~ 0.2 μm),
(b) sub-surface layer (from ~ 0.5 to ~ 2 μm), and
(c) bulk material (> 5 μm).

Deuterium concentration at high ion fluences ($\geq 1 \times 10^{24}$ D m^{-2}) decreases from several atom % in the near-surface layer to below 3×10^{-3} atom % in the bulk of both crystalline forms. Blister formation at high fluences accompanied by D release is observed for polycrystalline W, but not for W single crystals. D ion irradiation with ion energies well below the displacement threshold modifies the W structure to depths of up to about 5μm in both crystalline forms. These various observations can be attributed to plastic deformation of the W matrix caused by deuterium super-saturation within the near-surface layer. Deuterium retention depends strongly on the structure of the W materials, and the highest D concentrations were found in VPS W coatings. Sub-surface and bulk retention decreases in steps at elevated temperatures.

A.A. Haasz reported on studies of the erosion of carbon by tritium ions. Carbon-based materials have been extensively used in fusion research machines, and are under consideration for high heat flux components in ITER. Thus, measurements of the erosion rates of carbon from deuterium and tritium bombardment are of high priority in order to predict the lifetime of the components as well as tritium co-deposition (i.e., chemical erosion may be dominant under the relevant energies of ITER). Previous low-energy erosion measurements were undertaken by monitoring the behaviour of H and D, but not T. Thus, the objectives of the work have been to measure the rate of chemical erosion of graphite as a function of temperature by means of pure T beams at 10-500 eV energy, and to determine the distribution of released hydrocarbons. All experiments were performed in the UHV Tritium Laboratory with a pyrolytic graphite sample and a three-stage differential pumping system. Sample temperatures ranged from 300 to 950K. The resulting T_2^+ mass-analyzed beam decelerated to 50 to 500 eV/T^+ (after irradiation, thermal de-sorption showed the dominant species were T_2 and CT_4, confirming that the beam was T_2 with little H contamination). Chemical erosion yields of graphite for H^+, D^+ and T^+ were found to be very similar in their magnitude and temperature dependence. Other studies have shown no significant isotopic effects for H and D at higher energies that can also be reasonably assumed for T at tens of eV. Therefore, the measured erosion rates for H and D should provide suitable estimates for T as well.

V.Kh. Alimov reviewed work on deuterium retention in boron carbide (B_4C), which has been considered as a plasma-facing material (low Z-material, with high heat resistance and low chemical erosion). Deuterium retention was studied in sintered boron carbide samples irradiated with 3 keV D ions at room temperature or exposed to a low energy (~ 200 eV/D) and high ion flux (~ 10^{21} m^{-2} s^{-1}) D plasma at elevated temperatures. Under both ion irradiation and plasma exposure, deuterium is solely accumulated in B_4C as D atoms. At 300K, implanted deuterium accumulated mainly in the ion implanted zone. As the irradiation/exposure temperature increased, D atoms began to diffuse into the bulk. Above 600K and high fluences (greater than 10^{24} D m^{-2}), the bulk accumulation played a major role in D retention. At temperatures around 900K and high ion fluences, the maximum D concentration in the bulk (up to a depth of 50 μm) was ~ 0.1 atom %. The diffusivity of deuterium in sintered boron carbide was evaluated to be:

$$D = 1.4 \times 10^{-5} \exp\{-(100 \pm 10 \text{ kJ mol}^{-1})/RT\} \text{ m}^2 \text{ s}^{-1}$$

R. Causey reported on the behavior of tritium in tungsten. Tungsten has some desirable properties for use in fusion devices (e.g., ITER), including a very high melting point and high thermal conductivity. However, this material must not retain or permeate large quantities of tritium, and should not be released into the plasma. A review of the properties controlling the retention and release of hydrogen isotopes from tungsten shows that the retention of tritium in tungsten is typically quite small, and will not result in elevated inventories of tritium. While the blisters generated when tungsten is bombarded by energetic hydrogen ions are considered by some to be a potential problem, mitigating against the use of tungsten in fusion reactors, they can be prevented through careful manufacture and working of tungsten. The combination of a high melting point, high thermal conductivity, low tritium retention characteristics, and resistance to blistering supports the large-scale use of tungsten in ITER and other future fusion devices.

C.H. Skinner presented the results of studies on dust and deposition in NTSX. The possible formation of blisters in tungsten would reduced thermal contact within the bulk and could result in flaking, melting and evaporation under high heat loads. Generation of tungsten dust and radiological activation/dispersion are safety issues in assessments of plant accidents.

Tungsten samples blistered as a result of a high fluence of D-ions were subjected to an elevated heat flux from a scanning continuous wave Nd laser. Images taken during the laser heating revealed hot spots at the location of the blisters, showing that blister caps will experience much higher temperature excursions than an unblistered surface. Another segment of the work focused on measurements of temperature rise and morphological changes of graphite and CFC samples during exposure to a high heat flux. A scanning Nd laser was used to deliver pulses of high heat flux at pulse lengths of 1 to 200 ms. One key observation was that the thermal response of tokamak-generated co-deposits showed striking differences to the manufactured material. A third area of study involved the monitoring of dust deposits in NSTX by means of two quartz crystal microbalances. Time-resolved measurements were carried out over a 4-week period in which the net deposited mass of 13.3 μg cm^{-2} matched a value of 13.5 μg cm^{-2} measured independently by ion beam analysis. Monte-Carlo modelling suggests that transient processes are likely to dominate the mode of deposition. Since the amount of dust generated in next-generation machines is likely to scale up by two or three orders of magnitude as the erosion increases, dust will become a major factor in safety assessments, site licensing and tokamak operations. Dust particles that had accumulated on a view-port at the bottom of the NSTX vessel were examined with a digital optical microscope - Raman spectrometric analysis showed the particles to be disordered graphitic carbon (sp^2), easily recognized by the presence of the typical D-band at ~ 1330 cm^{-1} and G-band at 1585 cm^{-1}. Preliminary results from a novel electrostatic dust detector were also presented.

J.P. Coad reported on studies of tritium retention in JET, and methods of de-tritiation:

(a) Analysis of samples removed from the first wall of JET - before the 2001 shutdown, a known quantity of $^{13}CH_4$ was introduced (puffs) in order to follow the migration of carbon on a series of special tiles. Analyses were made of the films from various locations, and the resulting observations were presented, and further tiles were removed for analysis during the 2004 shutdown.

(b) Measurement of hydrogen retention during JET operations - deuterium retention was assessed for the tiles removed during the 2001 shutdown, and a trace tritium experiment was carried out in 2003.

(c) Development of techniques for improved temporal resolution of retention and deposition of hydrogen isotopes in JET - design and use of Quartz Micro-Balances (QMB) were described in detail (one prototype was installed in 2001, and additional units will be installed in 2004); details of these QMBs and results from studies in 2001-2004 have been published.

(d) Study of methods for in-vessel tritium inventory reduction – a photon-cleaning method was used to de-tritiate tiles *in-situ*. This procedure involves focusing intense UV and visible light from a flash-lamp by means of a parabolic reflector. Tiles of the inner divertor were treated at high power, and the deposited film was clearly seen to have been ablated from the surface, while a number of outer poloidal limiter tiles were to have been treated at lower power to out-gas the surface films without ablation (however, a problem developed with the lamp, so the treatment was carried out in the Beryllium Handling Facility at JET).

(e) Development of de-tritiation techniques for components removed from fusion devices - significant numbers of radioactive and Be-contaminated carbon tiles have been used in previous operational campaigns of JET and are now in storage.

A promising technique has been evaluated that involves sweeping the flame of an oxy-gas burner across a divertor tile to reach a temperature of ~ 1000K in ~ 500 s. Decontamination factors (DF) of 850 were achieved for whole tiles. Several smaller pieces of tile have also been treated under various burner conditions, such as number of runs and final temperature - one piece of tile reached a DF = 2500.

N. Bekris reviewed work on gamma irradiation of flakes retrieved from a fusion machine. During the DTE1 programme in JET, 35 g of tritium were injected. After an extensive de-tritiation campaign, approximately 3 g remained in the machine (probably within flakes). Approximately 150 g of flakes were collected. Tritium was released from the flakes at temperatures above 200ºC, but after heating to 800ºC only 89% of the tritium had been released (full combustion released the final 11%). The flakes also underwent a chronic tritium release at room temperature, proportional to the remaining tritium and thought to arise from the tritium decay process. Although tritium release is enhanced by heating, gamma radiation does not appear to have an effect. While gamma radiation also seems to have no effect on the O_2 release, the amount of water released is reduced after irradiation.

A. Pisarev described the removal of fuel from TEXTOR limiter tiles by means of a pulsed excimer laser:

(a) Preliminary investigations of laser-induced de-sorption of samples from the TEXTOR bumper limiter
- thermal de-sorption experiments demonstrated that deuterium is released in the low temperature range
- laser irradiations were performed at low power density below ablation threshold and demonstrated high de-sorption efficiency.

(b) Hydrogen retention in graphite and boron carbide
- hydrogen-ion implantation at energies of 100 eV and 1 keV was accomplished by means of a plasma discharge;
- thermal de-sorption spectra after implantation were used to measure hydrogen retention, and releases of H_2 and CH_4 were also monitored;
- accumulation of hydrogen was found to occur at very high fluences in the bulk material, and deep hydrogen transport was induced by implantation damage;
- small differences were observed between graphite materials, and a relatively smaller efficiency for crystalline B_4C was noted;
- releases of H_2 and CH_4 were compared: four peaks (or groups of peaks) at 500, 800, 1000, 1200K were typical for H_2, and one peak at about 800K was normal for CH_4.

(c) Hydrogen de-sorption from graphite in air has been investigated
- high temperature peaks decrease first (not observed for metals), and the release starts from deep layers (stimulated by the energy released due to recrystallization of damaged upper layers).

R.P. Doerner reported on US-EU studies of mixed materials. Results were presented from a collaborative programme between the USDOE and EFDA that has focused on the interaction of plasma materials with mixed C/Be/W structures. A systematic series of experiments were performed by exposing carbon and tungsten samples to deuterium plasmas seeded with controllable amounts of beryllium impurity ions. These studies focused initially on the erosion, deuterium retention and co-deposition properties of graphite exposed to beryllium-

containing deuterium plasmas. Even a very small concentration of beryllium impurity (as low as 0.2%) was sufficient to reduce the graphite target chemical and physical erosion rates dramatically. The cause of this reduction became apparent during post-exposure analysis of the graphite targets. Sample surfaces exposed at 200°C revealed essentially complete (> 90%) coverage of the graphite by a thin beryllium layer if the Be-seeding concentration exceeded 0.1%. Formation of beryllium-rich surface layers on the graphite targets also affected the re-deposited material that was found to consist almost entirely of beryllium, with only trace amounts of oxygen and carbon throughout most of the layer. The average deuterium content in this layer is consistent with previous retention measurements in 'clean' re-deposited beryllium at low temperatures. Although more hydrogen isotopes are retained during lower temperature co-deposition, they are more easily desorbed. The second investigation concerned Be interactions with tungsten - Be impurities from the ITER first wall form Be surfaces on the tungsten baffle plates, and can alloy with W to produce Be22W and Be12W alloys that have lower melting points (~ 1500°C). Thus, a W crucible with a Be ingot failed at a relatively low operating temperature of 1200ºC. These observations demonstrated that W-Be alloy formation is a critical issue requiring immediate attention (melt temperatures, thermal properties, formation rates, etc.).

Progress and results from all of the above work programmes have been well documented in published papers, and more detailed descriptions of the studies can also be found in Appendix 3.

3. Continuation of Work Plan

Detailed discussions took place on the specific areas in need of further research. Participants also formulated a specific work plan to address the major issues within the resources of the CRP. The following work plan was agreed for the necessary continuation of the CRP:

1. Identify sources and sinks in tokamaks using ^{13}C puffs
   - puffs using ^{13}C in ASDEX-UG will be monitored (J. Roth),
   - JET - ^{13}C tests have already been completed and were briefly reported; analyses of the tiles are in progress (J.P. Coad),
   - ^{13}C puffs are planned in DIII-D during 2005, and will be monitored (R.P. Doerner and A. Haasz),
   - ^{13}C puffs for JT-60 will be monitored (T. Tanabe).

2. Use of dopants (mainly Ti) has been examined during the course of this CRP – although measurements of their erosion rates and hydrogen retention have already been accomplished, this task will only be completed with the analysis of the eroded species (J. Roth).

3. Transport of hydrocarbon species in tokamaks - specialised erosion monitors (small boxes equipped with a small slit) have been installed in the divertor of JET and ASDEX-UG; they need to be removed, analysed and their data evaluated (M. Mayer and J.P. Coad).

4. A brief presentation was made of studies of C erosion and the dependence of this process on the amount of impurities (such as Be and W) – this work needs to be completed (R.P. Doerner).

5. Progress in the monitoring of the deposition of eroded material using Quartz Micro-Balances (QMBs) includes:
   - JET - QMBs are installed, and the work is still in progress (J.P. Coad),
   - NSTX - QMBs are being relocated, and plasma operations and deposition studies will recommence in February 2005 (C.H. Skinner).

6. Analyses of long-term samples are still on-going in all machines, and this work will be monitored as follows:
   - ASDEX-UG (J. Roth/M. Mayer),
   - JET (J.P. Coad),
   - JT-60 (T. Tanabe),
   - NSTX (C.H. Skinner).

7. Analysis of JET samples will be performed using the Neutron-induced Elastic Recoil Detection (NERD) - J.P. Coad will provide samples to S.V. Artemov.
   - Action: R. Causey to ensure S.V. Artemov gains contact with J. Knox.

8. The use of lasers as a removal technique and the evaluation of a possible re-absorption of the removed species will be investigated (A. Pisarev, T. Tanabe).

9. Other in-vessel techniques will be tested in different machines:
   - JT-60: de-tritiation using controlled amounts of H_2O amounts (T. Tanabe),
   - JET: tritium removal using flash-lamp photon cleaning (J.P. Coad) - efficacy of this technique will be assessed after the analysis of the photon-irradiated tiles (N. Bekris, J.P. Coad),
   - tritium removal using oxygen in JET (monitored by J.P. Coad) and DIII-D (monitored by R.P. Doerner and A. Haasz).

10. Require new de-tritiation proposals:
    - use of liquid nitrogen will be evaluated using JET and TFTR tiles (N. Bekris, R. Causey),
    - continuation of gamma irradiation studies as a possible de-tritiation technique for flakes and/or co-deposits (N. Bekris).

11. Effect of metal impurities with respect to thermal oxidation will be investigated using tokamak samples (A .Haasz) – J.P. Coad will provide the samples.

12. Laboratory oxidation studies of DIII-D and JET tiles will be investigated at the University of Toronto (A. Haasz).

13. Review of He/O_2 glow discharge provides a summary of all results published to date, and is almost finished (R. Causey).
    - ASDEX-UG results will be monitored and also included (J. Roth).

14. Studies of tritium retention on clean W will continue under various conditions (temperature and fluxes), and will also involve new analytical techniques such as Transmission Electron Microscopy (V.Kh. Alimov, R. Causey, R.P. Doerner).

15. Plasma-sprayed W exhibited higher deuterium retention than mono- or polycrystalline W – could be related to the crystallographic structure of the

material which needs to be determined. Face-centred cubic (fcc) W characterises the sputtered films deposited between 200°C and 400°C, but appears to be transformed to the normal body-centred cubic (bcc) structure after annealing at 700°C (R. Causey, R.P. Doerner):

- Action: G. Federici will provide samples.

16. Database of H retention on W is almost complete (R. Causey).

17. Modelling of tritium retention by means of TMAP7 (A. Pisarev):
    - Action: J. Roth and A. Haasz will try to obtain the code from G. Longhurst (INL, USA).

18. Presence of oxide and carbon layers on the W surface will be investigated, along with their influence on hydrogen permeation and retention under simultaneous C/H bombardment. (A. Haasz, J. Roth).

19. Diffusion of Be in W as a function of temperature and the formation of a Be-W alloy will be investigated. At temperatures not exceeding 600°C, Be does not react with W, but at higher temperatures the solubility of Be in W increases up to 3 atom %. Above 750/850°C, the formation of beryllides occurs (WBe_{12} and WBe_{22}); and at temperatures exceeding 1000°C, only WBe_{22} is observed. Such alloys are very brittle (R. Doerner), and therefore their formation could be a critical issue for ITER (R. Causey, R.P. Doerner, J. Roth).

20. The injection of Be into the plasma and retention by a W substrate will be studied (R. Causey, R.P. Doerner).

21. Generation of data for hydrogen retention by tungsten carbides such as WC and W_2C is in progress (V.Kh. Alimov).

22. Both the diffusion and retention of hydrogen in metal films such as W or Al (as well as in carbon metal films) will be studied, with the aim of modelling the behaviour of Be (A. Pisarev).

Additional activities related to CRP:

R. Causey:	H/He retention and release by liquid metals.
A. Haasz:	H retention in W under simultaneous H^+/He bombardment.
N. Yoshida:	He effect on H retention in PFC materials: W, Mo and V.
T. Tanabe:	Tritium imaging of Tokamak tiles.
V.Kh. Alimov:	Deuterium retention in W pre-irradiated with hydrogen and He ions. Continue measurements on the deuterium retention in B_4C after exposure of B_4C to deuterium gas.
S.V. Artemov:	Change the existing design of the experimental set-up, and continue improvements to the sensitivity and depth resolution of NERD including: modifications to fast gate module, change design of neutron target device.
J.P. Coad/N. Bekris:	Tritium removal (by heating) from flakes collected at JET.
C.H. Skinner:	Compare results obtained for the corresponding experiment with TFTR flakes (see above).
N. Bekris:	Assess tritium content of complete JET tiles by means of calorimetry.

4. Concluding Remarks

The CRP on "Tritium inventory in fusion reactors" has successfully achieved all of the objectives established at the beginning of the initial phase of the project. Furthermore, all participants have published their work in refereed journals over the course of the CRP, are in the process of making their data available in electronic form, and have prepared summaries of the research performed to date. Under these extremely productive circumstances, a detailed work plan has been formulated to continue these important CRP studies into 2006.

Appendix 1

Second IAEA Research Co-ordination Meeting on
Tritium Inventory in Fusion Reactors

18-19 October 2004, IAEA Headquarters, Vienna, Austria

List of Participants

Dr. A.A. Haasz
Professor and Director
University of Toronto
Institute for Aerospace Studies
4925 Dufferin St.
Toronto, Ontario M3H-5T6
CANADA
Tel.: +1-416-667-7734
Fax: +1-416-667-7743
E-mail: aahaasz@utias.utoronto.ca

Dr. N. Bekris
Forschungszentrum Karlsruhe
Central Experimental Department
P.O. Box 3640
D-76021 Karlsruhe, GERMANY
Tel.: +49-7247-82-2932
Fax: +49-7247-82-2868
E-mail: nicolas.bekris@hvt.fzk.de

Dr. J. Roth
Max-Planck-Institut für Plasmaphysik
Boltzmannstrasse - 2
D-85748 Garching bei München
GERMANY
Tel.: +49-89-3299-1387
Fax: +49-89-3299-1149
E-mail: roth@ipp.mpg.de

Dr. Tetsuo Tanabe
Center for Integrated Research in
Science and Engineering
Nagoya University
Furo-cho, Chikusa-ku
Nagoya 464-8603
JAPAN
Tel.: +81-52-789-5157
Fax: +81-52-789-5177
E-mail: tanabe@cirse.nagoya-u.ac.jp

Dr. V.Kh. Alimov
Institute of Physical Chemistry
Russian Academy of Sciences
Leninsky Prospect 31
119991 Moscow
RUSSIAN FEDERATION
Tel.: +7-095-330-2192
Fax: +7-095-334-8531
E-mail: alimov@ipc.rssi.ru

Dr. Alexander Pisarev
Moscow State Engineering and
Physics Institute
Kashirskoe sh. 31
115409 Moscow
RUSSIAN FEDERATION
Tel.: +7-095-323-9321
Fax: +7-095-324-7024
E-mail: pisarev@plasma.mephi.ru

Dr. J.P. Coad
Room K1/0/13
United Kingdom Atomic Energy
Authority (UKAEA)
Culham Science Centre
Abingdon
Oxon, OX14 3DB
UNITED KINGDOM
Tel.: +44-1235-464478
Fax: +44-1235-464535
E-mail: paul.coad@jet.uk

Dr. Rion A. Causey
Sandia National Laboratories
MS 9402
P.O. Box 969
Livermore, CA 94550
U.S.A.
Tel.: +1-925-294-3326
Fax: +1-925-294-3231
E-mail: causey@ca.sandia.gov

Dr. Russell Doerner
Rm. 460, EBU-II
University of Califoria, San Diego
UCSD Fusion Program
Experimental Research Division
9500 Gilman Dr.
La Jolla, CA 92093-0417
U.S.A.
Tel.: +1-619-534-7830
Fax: +1-619-534-7716
E-mail: rdoerner@ferp.ucsd.edu

Dr. Charles H. Skinner
MS 15
Princeton Plasma Physics Laboratory
Route 1 North
P.O. Box 451
Princeton NJ 08543
U.S.A.
Tel.: +1-609-243-2214
Fax: +1-609-243-2665
E-mail: cskinner@pppl.gov

Dr. Sergey Artemov
Institute of Nuclear Physics
Uzbekistan Academy of Sciences
Ulugbek, Tashkent 702132
UZBEKISTAN
Tel.: +998-712-606657
Fax: +998-712-642590
E-mail: sartemov@suninp.tashkent.su

Dr. R.E.H. Clark
IAEA Atomic and Molecular Data Unit
Wagramerstrasse 5
P.O. Box 100
A-1400 Vienna
AUSTRIA
Tel.: +43-1-2600-21731
Fax: +43-1-26007
E-mail: r.e.h.clark@iaea.org

Dr. D. Humbert
IAEA Atomic and Molecular Data Unit
Wagramerstrasse 5
P.O. Box 100
A-1400 Vienna
AUSTRIA
Tel.: +43-1-2600-21729
Fax: +43-1-26007
E-mail: d.humbert@iaea.org

Appendix 2

Second IAEA Research Co-ordination Meeting on
Tritium Inventory in Fusion Reactors

18-19 October 2004, IAEA Headquarters, Vienna, Austria

Agenda

Monday 18 October **Meeting Room: F-01-21**

09:30-10:00 Opening, Adoption of Agenda, A. Nichols, R. Clark

Session 1: Progress Reports I

Chairman: A. Pisarev

10:00 – 10:30 T. Tanabe
Retention of hydrgen isotopes and carbon deposition

10:30 – 11:00 *Coffee Break*

11:00 – 11:30 S. Artemov
NERD-Method for Study of the Profiles of Tritium Concentration in Interior Elements of Fusion Reactors

11:30 – 12:00 J. Roth
Deuterium Retention in W Materials by depth profiling up to 7 μm

12:00 – 12:30 A.A. Haasz
Erosion of carbon due to tritium ions

12:30 – 14:00 *Lunch*

Session 2: Progress Reports II

Chairman: T. Tanabe

14:00 – 14:30 V. Alimov
Deuterium retention in boron carbide

14:30 – 15:00 R. Causey
Behavior of tritium in tungsten

15:00 – 15:30 C. Skinner
Dust and deposition in NSTX

15:30 – 16:00 *Coffee Break*

16:00 – 16:30 J.P. Coad
Studies of tritium retention in JET and of de-tritiation

16:30 – 17:00 N. Bekris
Gamma irradiation of flakes retrieved from a fusion machine

17:00 – 17:30 A. Pisarev
Fuel removal from TEXTOR limiter tiles by using a pulsed excimer laser

17:30 – 18:00 RDoerner
US-EU collaboration results on mixed-materials

Tuesday 19 October

Session 3: Review of work plan and outcomes

Chairman: J. Roth

09:00 – 12:30 All
Comprehensive review of results obtained in support of the work plan for the CRP and formulation of conclusions

12:30 – 14:00 *Lunch*

Session 4: Formulation of work plan for extension of CRP

Chairman: N. Bekris

14:00 – 17:00 All
Formulation of work plan for extension to CRP with final RCM in 2006

17:00 *Adjournment*

Appendix 3

Second IAEA Research Co-ordination Meeting on
Tritium Inventory in Fusion Reactors

18-19 October 2004, IAEA Headquarters, Vienna, Austria

Summaries from Participants

Deuterium Retention in Boron Carbide

V.Kh. Alimov

Institute of Physical Chemistry, Russian Academy of Sciences

Leninsky prospect 31, 119991, Moscow, Russia

Boron carbide B_4C is considered a potential plasma facing material for fusion reactors due to its low atomic number, plasma compatibility, high melting point and low chemical erosion yield. Because of its low atomic number, this ceramic is expected to reduce plasma contamination. Due to its refractory character it can operate at high temperatures. Data on hydrogen isotope retention in boron carbides are importat for the application of boron carbide materials in fusion related plasma devices (DIII-D, Wendelstein 7-X). There are few data available on the temperature dependence of D retention in B_4C: The present work was undertaken to provide information on deuterium retention in B_4C samples (i) irradiated with D ions, (ii) exposed to a low-energy and high flux D plasma and (iii) exposed to D_2 gas at different temperatures.

Sintered boron carbide B_4C supplied by Wacker-Chemie GmbH, Kempten, Germany was used to study deuterium retention in the material. The B_4C samples were irradiated with 3 keV D ions at room temperature or exposed to a low energy (~200 eV/D) and high ion flux (~10^{21} $m^{-2}s^{-1}$) D plasma at elevated temperatures. Additionally, the B_4C samples were exposed to D_2 gas at pressures of 0.1 and 1 Pa at temperatures in the range from 553 to 1143 K. The $^3He + D$ nuclear reaction at different ^3He energies, secondary ion mass spectrometry and residual gas analysis (SIMS/RGA) methods were used for quantitative deuterium depth profiling.

SIMS/RGA measurements showed deuterium is accumulated in B_4C as D atoms solely both under the ion irradiation and plasma exposure.

After irradiation with 3 keV D ions at 300 K to a fluence of 7.5×10^{20} D/m^2, the deuterium concentration remains unaltered with time of aging in air. But after a fluence of 7.5×10^{22} D/m^2, the pronounced tendency to the D concentration decrease and the oxygen content increase with time of keeping in air is observed. The development of open porosity in the ion implanted zone and water vapor interaction with B_4C molecules and superstoichiometric boron atoms accompanied by formation of volatile boron-deuterium compounds are thought to be main mechanisms of oxygen accumulation and deuterium release.

In the B_4C samples exposed to the D plasma at temperatures in the range 553 to 923 K, D atoms diffuse into the bulk (up to a depth of 10 μm) and accumulate up to a maximum concentration of ~0.2 at.%. At high fluences (≥ 10^{24} D/m^2), the accumulation in the bulk plays the major role in the D retention (Fig. 1). With increasing exposure temperature, the amount of D retained in B_4C increases and exceeds a value of 1×10^{22} D/m^2 at 923 K.

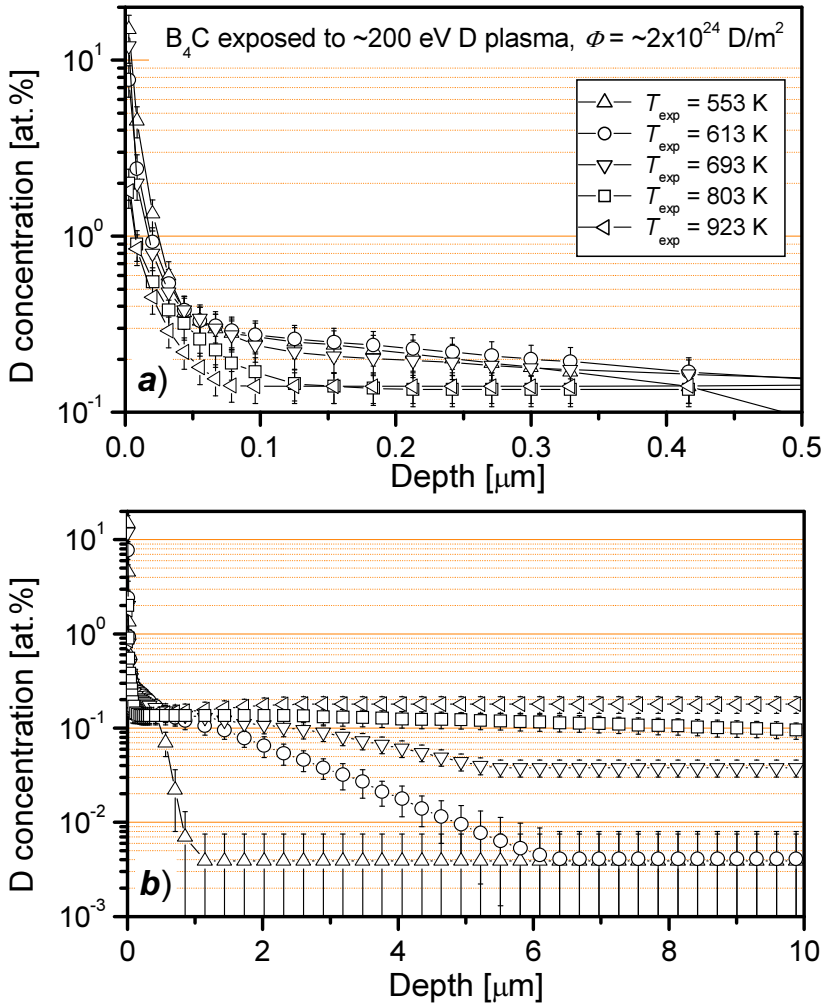

Fig. 1. Depth profiles of deuterium trapped in the near-surface layer (a) and in the bulk (b) of B_4C exposed to a low-energy (≈200 eV/D) deuterium plasma to a fluence of about 2×10^{24} D/m^2 at different temperatures. The D concentration up to 0.5 μm (a) was determined from the energy spectra of α particles emitted from the D(^{3}He,α)H reaction. Note that the depth and concentration scales in parts (a) and (b) are different.

There are two channels for deuterium diffusion. A "fast" diffusion channel allowing the penetration of D atoms deep into the bulk (at least up to a depth of 10 μm) even at T_{exp} = 553 K, and resulting in the formation of the flat-shaped D profile with concentrations of ~4×10^{-3} at.% at 553-613 K and ~4×10^{-2} at.% at 693 K. A "slow" diffusion channel provides the gradient of the deuterium profiles from a maximum concentration of 0.1-0.2 at.% into the bulk. In the "slow" channel the deuterium diffusivity is estimated to be $D = 2.6\times10^{-6}$ exp{-(107±10 kJ mol^{-1})/RT} m^2 s^{-1}.

In the course of the D_2 gas exposure, the D amount increases initially and then decreases as the exposure temperature increases. The maximum amount of deuterium atoms retained in the B_4C samples after the D_2 gas exposure at a pressure of 0.1 Pa for 2 h is ~9×10^{18} D/m^2, and this value is reached at T_{exp} = ~1000 K. At the D_2 pressure of 1 Pa, the amount of deuterium atoms sorbed in the B_4C sample for 30 min reaches its maximum value of ~3×10^{19} D/m^2 at T_{exp} = ~700 K.

NERD-method to study profiles of tritium concentration in interior elements of a fusion reactor

S.V. Artemov, Ya.S. Abdullaeva, A.H. Abdurakhmanov, A.A. Karakhodzhaev, G.A. Radyuk, V.P. Yakushev, E.A. Zaparov

Uzbekistan Academy of Sciences
Institute of Nuclear Physics, Uzbekistan

Features of the method:

- Nondestructive method of study.
- All hydrogen isotopes are analyzed simultaneously.
- Possibility of the analysis irrespective to the condition of material (gas, liquid, solid).
- Maximal depth of the analysis is defined by the range of recoiled nucleus in material (~ 0.1 – 1 mm).

Measurement by means of the NERD method:

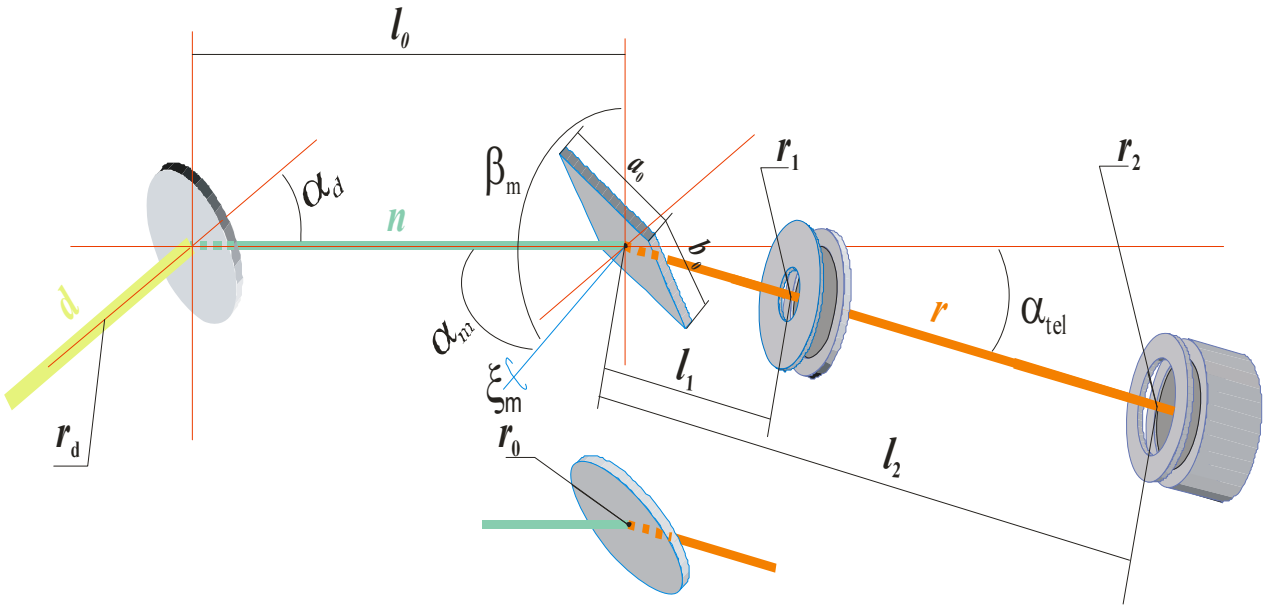

Design and manufacturing of the elements inside the NERD reaction chamber:

To increase the sensitivity (detection limit) of the method, we need firstly to decrease the background count rate:

- sources are the reactions induced by fast neutrons on the constructive materials around the detector telescope.
- detectors work in a gamma-radiation field conditioned by the neutron flux (dominating source of this gamma-radiation is the tritium target).

Other sources of gamma background are the constructional material of the scattering chamber and inner elements. This part of the background may be reduced by choice of a material with smaller cross-section for gamma-ray generation and by reduction of amount of material.

The cross-sections for γ-quanta generation are given in Fig. 1 for some nuclides that are included in the various constructional materials [5]. They are minimal for C, Al and Si nuclides. Taking into account constructional and technological reasons, we come to a conclusion that the aluminum alloys are preferable for the scattering chamber and inside elements. This work is planned for the future.

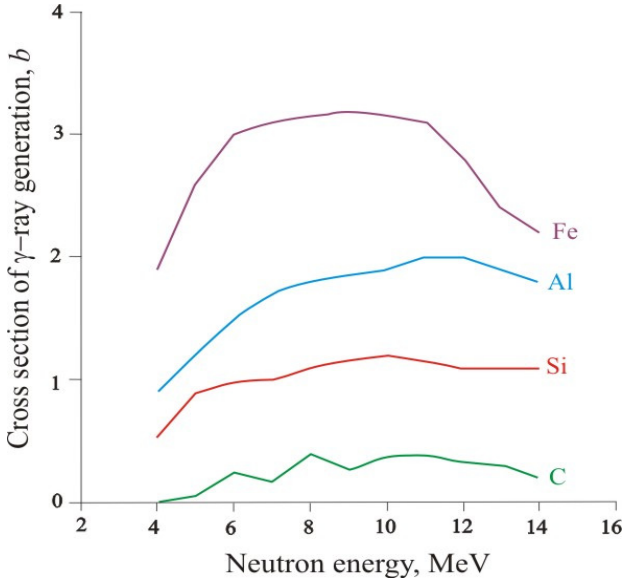

Fig 1. Total cross-sections of gamma-ray generation by neutrons in carbon, aluminum, silicon and iron, as a function of neutron energies.

The design of the telescope requires great care. We made a selection of materials that may be used as constructional ones, taking into account (*n, charged particle*) reaction cross sections - the box of the telescope, diaphragms and cells of the detectors should be manufactured from carbon.

Carbon is a unique material, with a small proton yield (cross section of (*n, p*) reactions on ^{12}C is 0.19 mb [4], reaction energy $Q = -12.6$ MeV). So, at the energy of neutrons $E = 14.1$ MeV (generated by NG-150), protons have an energy of 1.5 MeV, insufficient to pass through the first ΔE-detector. The energy of the (*n, d*) reaction on carbon is even higher at 13.7 MeV. The energy of the (*n ,t*) reaction on carbon is 18.9 MeV. Thus, the threshold of the (*n, t*) reaction is higher that the energy of the neutrons, and reduces the background sufficiently. As it is shown above, carbon also has a small cross section for the gamma-quantum generation. Diaphragms and a new box for the telescope (Fig. 2, left) have been manufactured from graphite. Fig. 2 (right) shows a variant of the telescope as assembled. The box of the telescope was arranged so that the detectors see nothing except carbon and the material of the analyzed sample. In both cases, the background of the charged particles and gamma-radiation are minimal. The neutron flux passes through the flange of neutron target device, entrance window of the scattering chamber and sample holder before hitting the sample. As a result of scattering, the neutrons undergo additional energy spread. Therefore, the material with minimal cross section for neutron elastic scattering should be used. Taking into account the design reasons, the most appropriate candidates are iron and aluminum alloy that contain significant amounts of Si. For an aluminum alloy (80% of Al and 20% of Si), the cross section for neutron scattering at the region of zero degree is 1.28 barn/sr (factor of 2.3 times less than that of iron [5]).

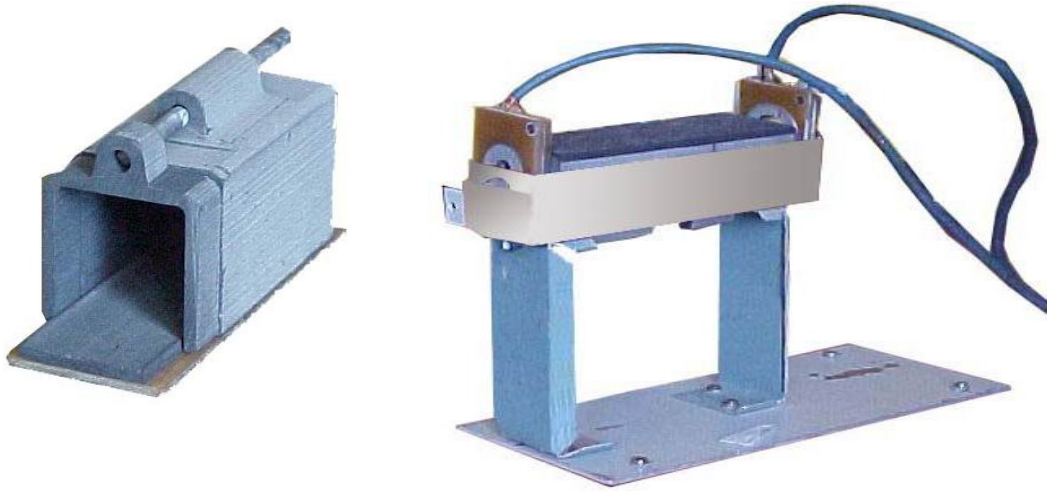

Fig. 2. Telescope of detectors - detector cells are pulled out, and the analyzed sample is displaced. Telescope made of graphite is shown on the left-hand side.

A new entrance window of the scattering chamber has been made of a sheet of aluminum alloy (window diameter of 32 mm; thickness of 0.7 mm). Moreover, a new design of neutron target device will be developed to reduce escaping scattered neutrons. The effect of reducing the neutron scattering by steel is demonstrated by two experimental recoil proton spectra ("sandwich" sample) – see Fig. 3. Upper Fig. 3: neutrons pass through flange of target device (angle α_d "deuteron beam – neutron trajectory" ~ 90°) Lower Fig. 3: neutrons pass by flange of target device (angle α_d "deuteron beam – neutron trajectory" ~ 65°, far from the optimal one).

Optimization of the depth profile resolution and time of measurement using Monte-Carlo simulation

The energy spread of neutrons, energy resolution of the detectors, and the measurement geometry contribute to the total energy resolution of the recoil spectra, and may be reduced**:**

i) As shown in Ref. [6], neutrons that escape from the neutron target under angle 95^o relatively to the primary deuteron beam have minimal energy dispersion connected with the kinematical spread (≈ 90 keV/degree) - the new design of target device allows measurements under that angle.
ii) Effect of the measurement geometry was analyzed by simulating the physical processes by means of the Monte-Carlo method. The geometry of the spectrometer is shown in Fig. 4.

Monte-Carlo simulations have been carried out for various geometry parameters that are shown in Fig. 5. The telescope diaphragms are: r_1 = 4 mm, r_2 = 8 mm (^{1}H recoils are considered). Thus, R_1 and R_2 regions in Fig. 6 are separated by lines of equal energy resolution (on the right, in terms of MeV) and equal count rate (below, in arbitrary units). This diagram allows one to choose the proper energy resolution and count rate of a spectrometer.

Let us compare two variants of the spectrometer geometry: $R_1 = R_2$ = 150 cm and $R_1 = R_2$ = 100 cm. The first variant corresponds to the best energy resolution (120 keV), while the energy resolution for the second variant is 350 keV.

One should also mention that the improvement in the energy resolution is achieved by increasing the exposition time by a factor of five.

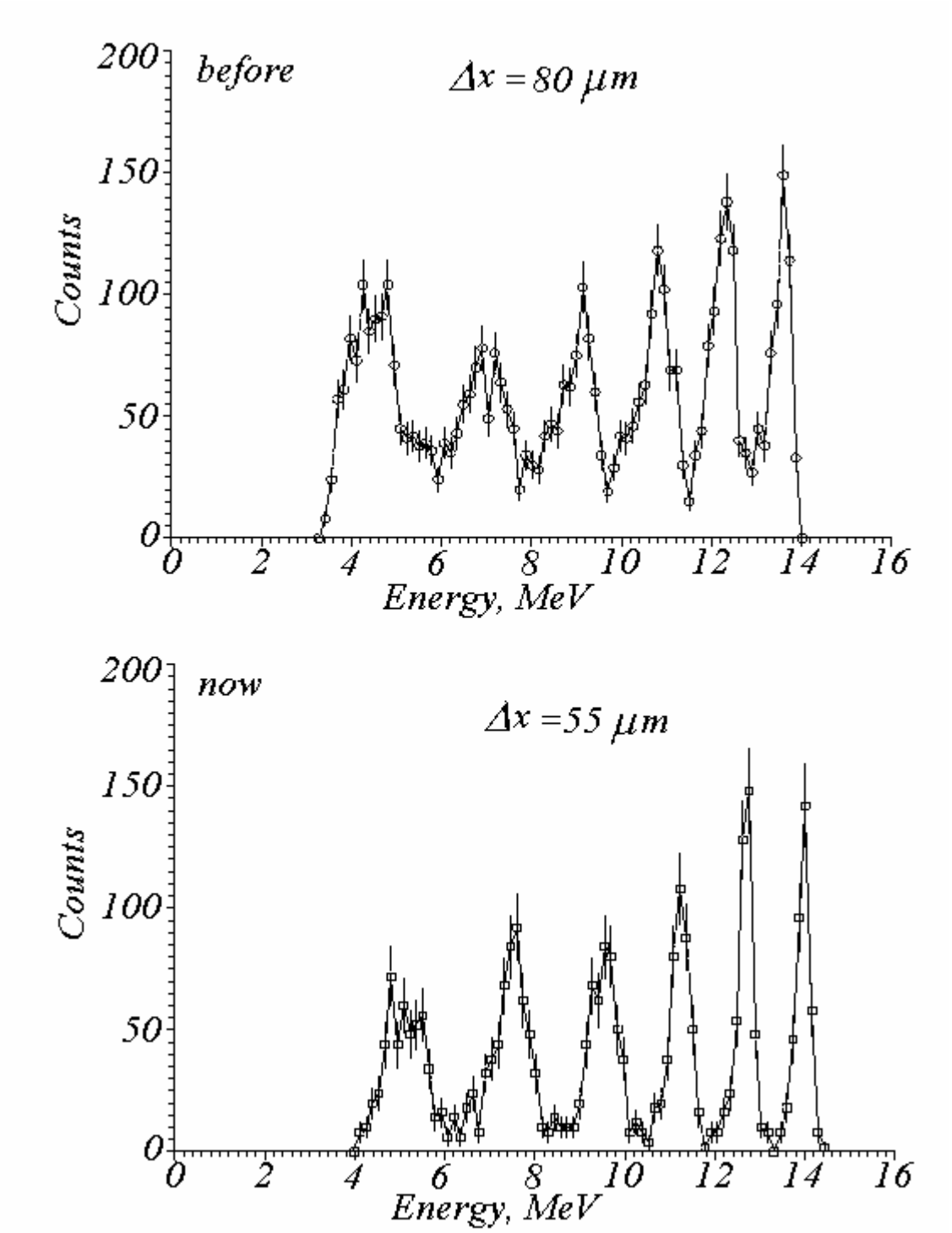

Fig. 3. Experimental recoil proton spectra.

Spectrometer modifications:

- Ti-T neutron target is an intensive source of gamma irradiation, and can not be dismissed in principle,
- fast spectrometric electronics are needed to avoid pulses superposition,
- new spectrometer based on two-detector telescope was developed for this purpose.

For minimization of the false coincidences quantity and for elimination of worsening of the energy resolution as conditioned by this background [2], we turned down traditional build-up of the spectrometer as a fast-slow arrangement of the circuit, and used only the fast branch of the electronics down to the last spectrometric amplifier before amplitude-digital conversion.

The "geometrical" energy spread of recoils ΔE_g is defined by the sizes of the telescope apertures and the neutron beam spot on the analyzed sample. The main parameter that defines the value ΔE_g is the angle $\Delta\vartheta_{max}$ of maximal deflection of the charged recoils (*p, d, t*) knocked out from the sample by the neutron and detected by the telescope:

$$\Delta E_g = E \cdot \sin^2 \Delta\vartheta_{\max}$$

where

$$\Delta\vartheta_{\max} = r_1 / R_1 + r_2 / R_2$$

The values of the "geometrical" energy resolution can be obtained for various sets of geometrical parameters of a telescope.

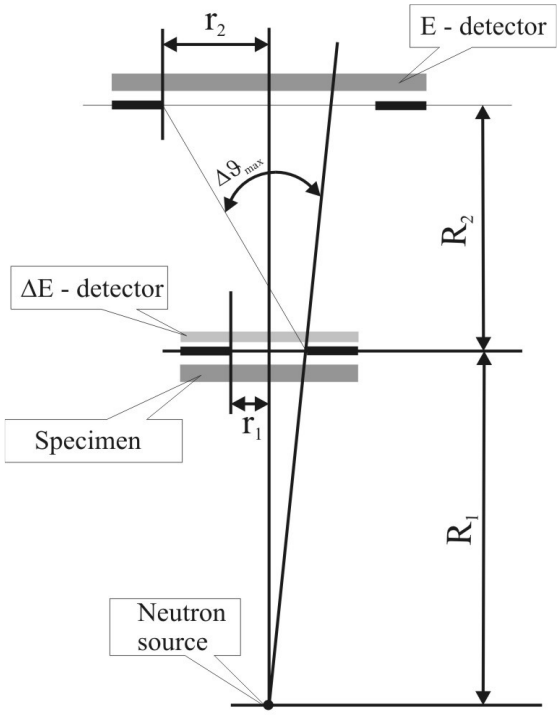

Fig. 4. Geometry of the spectrometer - a specimen is situated as close as possible to the first ΔE detector.

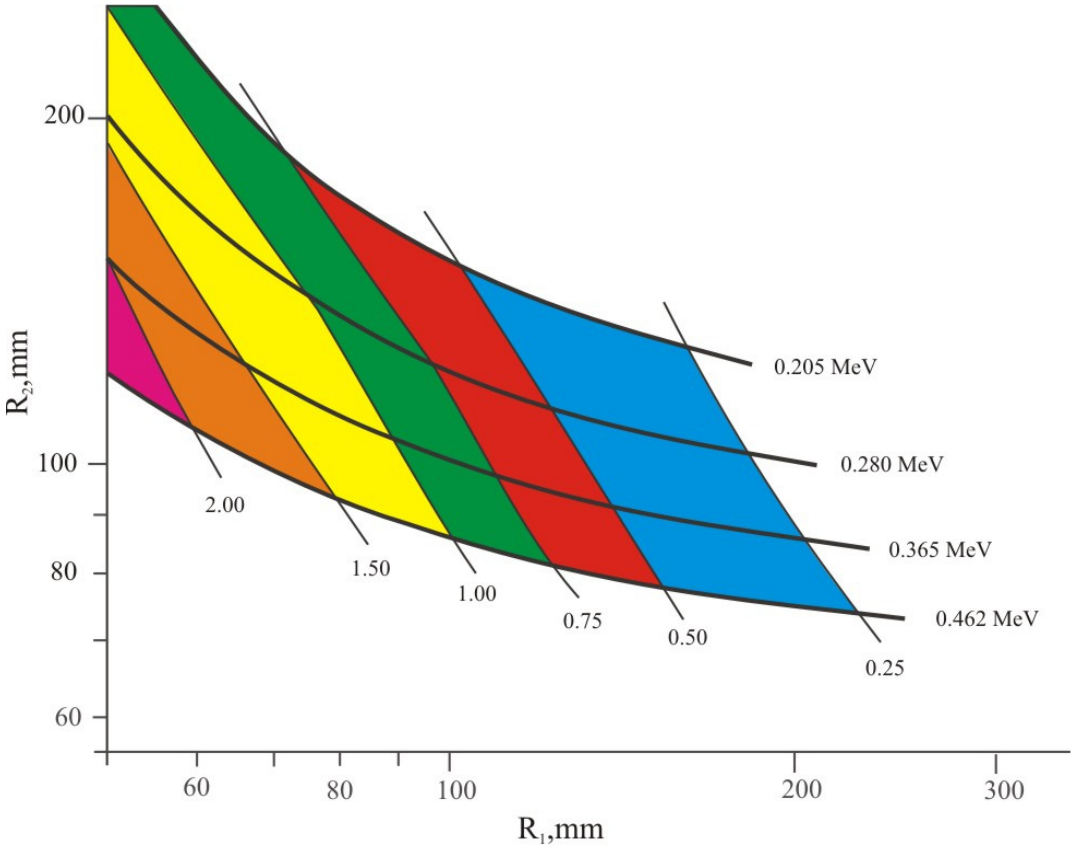

Fig. 5. Topography of the energy resolution and count rate calculated for apertures of ΔE and E-detector ∅8 and ∅16 mm, respectively.

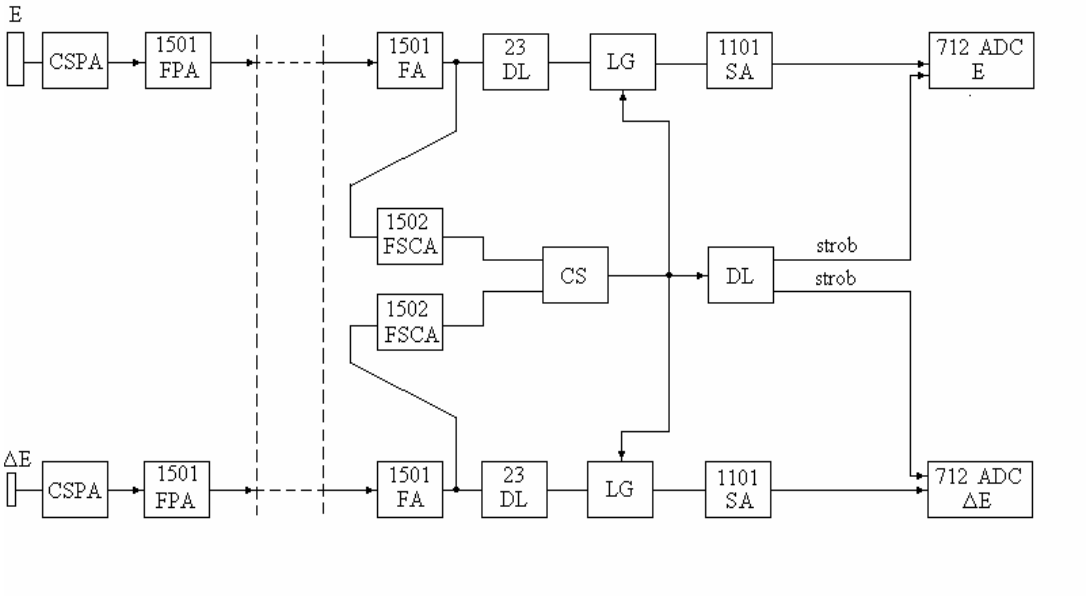

Fig. 6. Block diagram of the spectrometer.

1501 FA, FPA - fast amplifier (fast post-amplifier); 1502 FSCA - fast discriminator (single-channel analyzer); 23 DL- cable delay line; 1101 SA- spectrometric amplifier; 712 ADC (E,ΔE)- analog-to-digital converter; CSPA - charge-sensitive preamplifier with a fast output; CS – fast coincidence scheme; LG - linear gate; DL – delay line.

Distinctive feature of the spectrometer is the use of a fast output signal of the charge-sensitive preamplifier, permitting operation at large pulse loads. The specified innovation has allowed the use of two-detector system of (ΔE − E) for charged particles identification instead of the three-detector telescope which has been used before.

Blocks marked out by numbers (and letters) in the scheme are standard CAMAC modules (Fig. 6); blocks marked out by letters are the original units designed for the spectrometer.

The spectrometer operates in the following manner:

- Fast ΔE and E signals of CSPAs are shaped and gained by the amplifiers 1501; they are then transmitted through a cable in the measuring room, where they are shaped and gained again by other amplifiers 1501 for optimal operation of the fast discriminators 1502 and the linear gates LG. Discriminators 1502 generate logic signals for the coincidence scheme CS.
- If within a limit of 50 ns there is a coincidence of ΔE and E signals, CS produces the logic signal which opens an input of the linear gates LG, and the spectrometric signal is transmitted to the spectrometric amplifier 1101.
- The amplifier shapes and gains short signals passed through LG to adapt the shape of pulses for an input of the ADC.
- Delay line DL allows synchronization of the spectrometric signals and gating signal (strobe) for ADC operating.
- Pulse stretchers and analogous summing units of ΔE and E signals are excluded in the spectrometer.

Summation and treatment of the (ΔE + E) signal is carried out by means of the NERD-EDE program, which has been developed for the given spectrometer.

Assembly and fine adjustment of the spectrometer

Figs. 7 – 10.

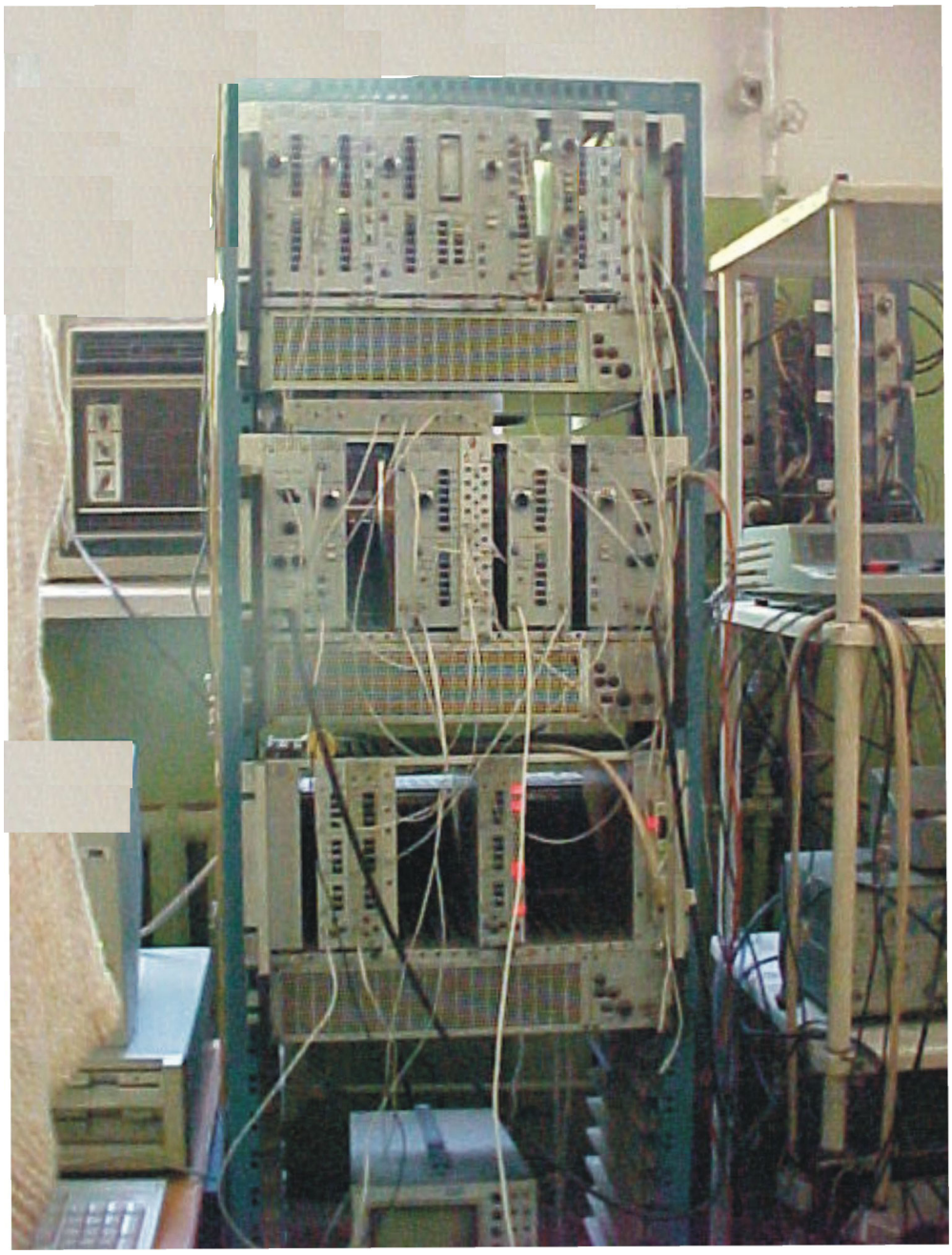

Fig. 7. Spectrometer assembly.

All electronic modules are adjusted on impedances and time synchronisation. The shapes of pulses of spectrometer fast units are shown in the following figures.

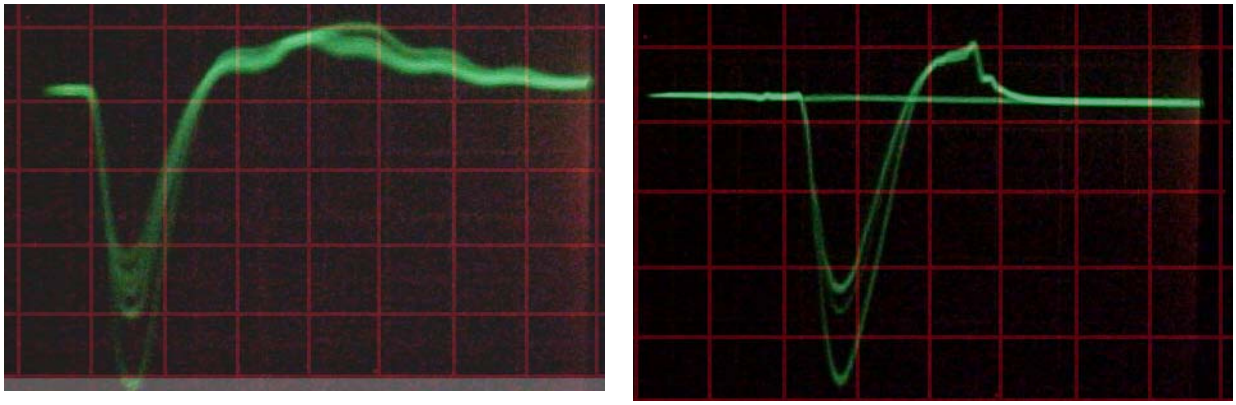

Fig. 8. Pulse shape of fast amplifier (left) and fast gate output signals - rise time of the pulse is 70 ns.

One can see from these figures that the time resolution of the selection of events in the fast part of the spectrometer is about 100 ns. The pulses before the amplitude analysis are shaped and have larger rise time. Shape of the pulse is shown in Fig. 11.

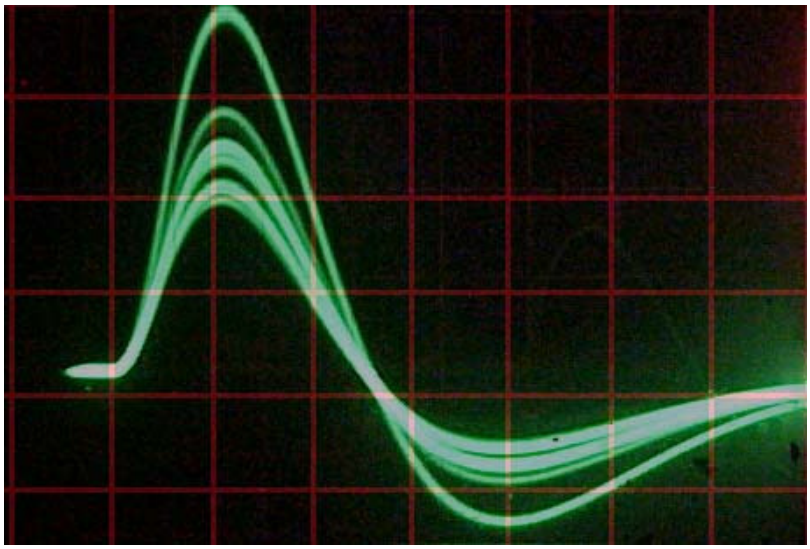

Fig. 9. Shape of pulses on output of the spectrometric amplifier 1101 - rise time of the pulse is 1 μs.

Forming of the energy spectrum is made on the following principle. The software for measurement carrying out is created as basic program NERD-EDE and of some small service programs. Program NERD-EDE carries out accumulation of the spectrometric information, processing, adjustment and service functions, and supports the standard graphic interface with the user. A specific feature is the opportunity of accumulation of the information at high loading of the spectrometer [5].

The procedure of the spectrometric information accumulation allows to build in memory of a computer both two-dimensional (ΔE, E) and linear spectra corresponding to various groups of registered particles.

Finally, Fig. 10 illustrates the working display of the whole spectrometer. The energy spectrum of alpha-particles from a Ra-226 α-source is shown, together with the menu of the NERD-EDE program.

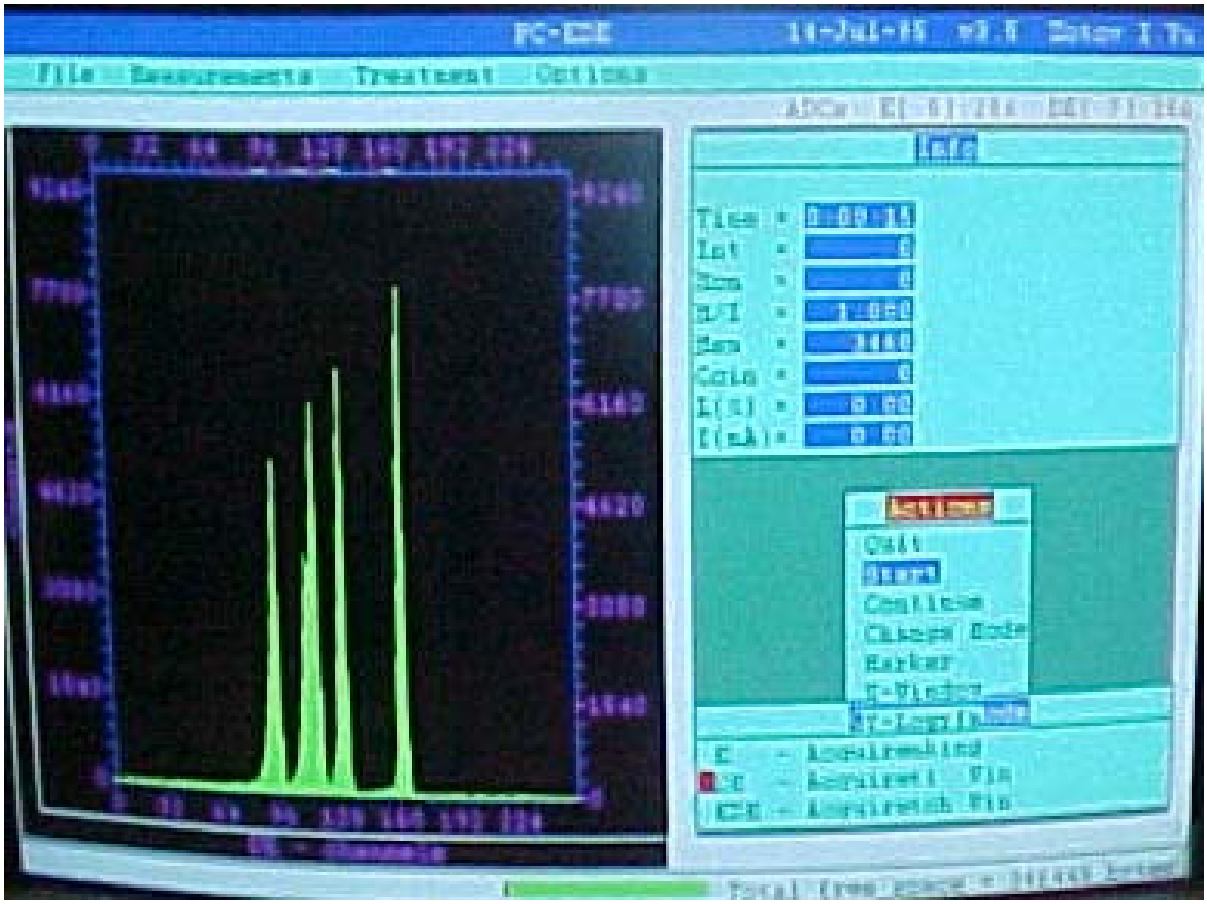

Fig. 10. Energy spectrum of alpha particles.

Evaluation of the parameters of the NERD device using the model samples

Using the Monte-Carlo simulation program allows one to undertake a preliminary evaluate of the main characteristics of the modified NERD spectrometer [6], and the special (model) samples were analyzed.

Fig. 11 shows the simulated energy spectrum of the recoiled protons for the model sample of six hydrogen-containing films (thickness of CH_2 films is 1 mkm) alternated by aluminum layers (thickness 180 mkm). The resolution of the detectors is 100 keV, and a telescope with good "geometrical" resolution (120 keV) is assumed in all of the tests.

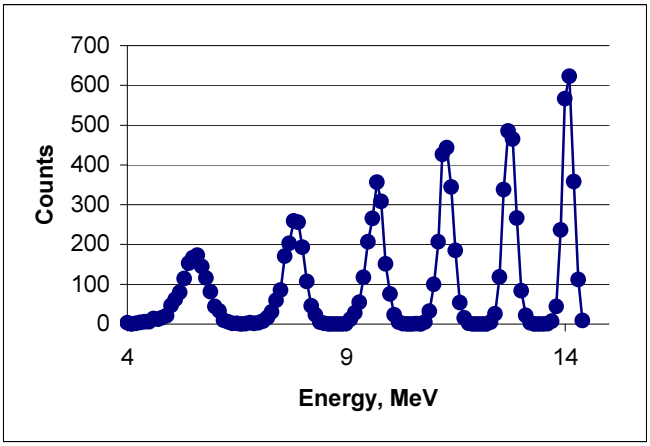

Fig. 11. Simulated energy spectrum of protons - neutron irradiation of a complex hydrogen-containing sample consisting of six films of CH_2.

Depth resolution can be evaluated when the energy spectrum of recoils is simulated for the sample in which two thin hydrogen-containing layers (each a thickness of 1 mkm) separated by aluminum layer (thickness 60 mkm) are situated on both sides of the aluminum plate of thickness of 800 mkm. This simulated experiment reproduces the depth distribution of hydrogen correctly in the model sample, and allows one to estimate the depth resolution of NERD spectrometer as 50 mkm.

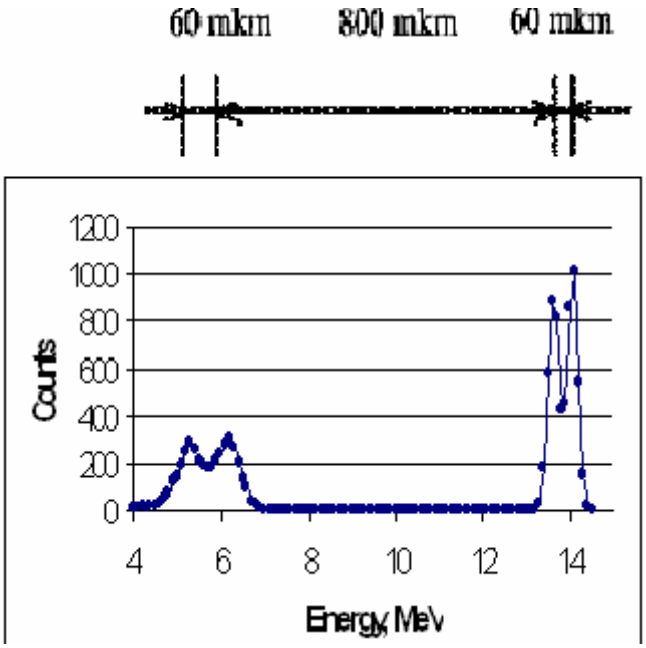

Fig. 12. Energy spectrum of protons simulated for a sample containing short-distance hydrogen-containing layers of CH_2.

Such simulation has been carried out for the complex titanium sample, containing thin tritium layers. Tritium layers (TiT) with thickness of 1 mkm are located at different depths of the titanium sample with distance between them of 15, 20 and 25 mkm. The depth resolution of tritium is obviously not worse than 15 mkm within a total depth of the complex titanium sample with thickness 100 mkm.

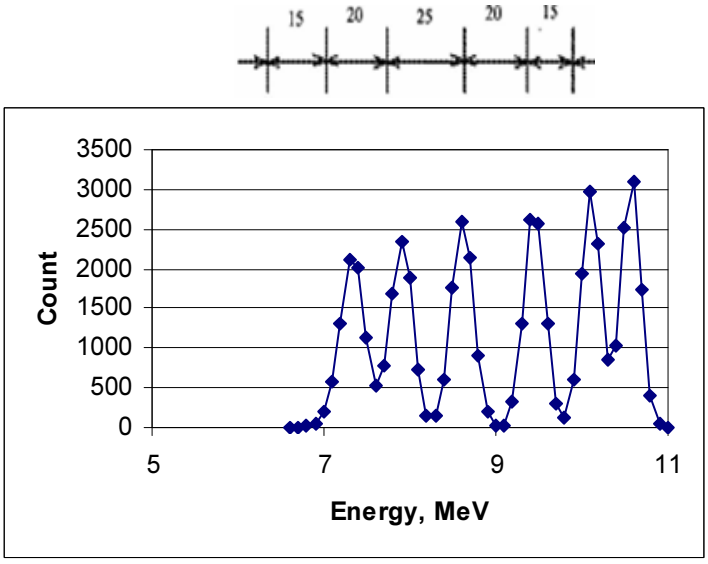

Fig. 13. Energy spectrum of tritons simulated for a complex titanium sample that contains TiT layers.

Same as above, but the telescope resolution is supposed to be negligible. So the best accessible depth resolution (FWHM) is ~ 5 mkm.

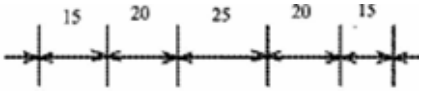

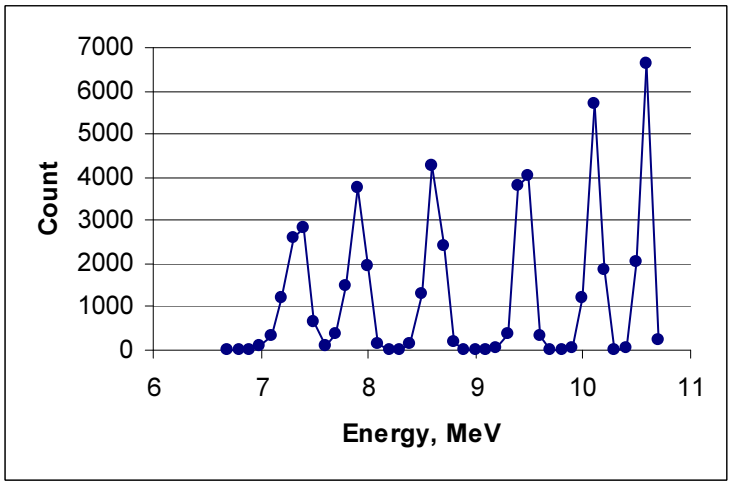

Testing of the spectrometer using model specimens

We present the energy spectra of tritons and deuterons obtained from measurements on two samples. As a sample, we used titanium-tritium targets (TiT_2) and used the neutron generator to produce a flux of fast neutrons. These samples side-by-side with the tritium contain the deuterium that collected as a result of the deuteron bombardment.

Depth distributions of these isotopes were obtained by simulation of the recoil energy spectra using the software developed by us.

Fig. 14 illustrates the energy spectrum of tritons (measurement № 527). As the energy spectrum is symmetrical, we can conclude that the tritium is uniformly distributed through the titanium layer. Calculated spectra of tritons (when the geometrical part of the total energy resolution is equal 300 keV and the energy resolution of detectors equals 120 keV) are shown in Fig. 15 for three supposed thicknesses of 20, 25 and 30 microns occupied by tritium. These data show that the calculated curve best fits the experimental distribution when the thickness of the tritium layer is assumed to be 25 microns.

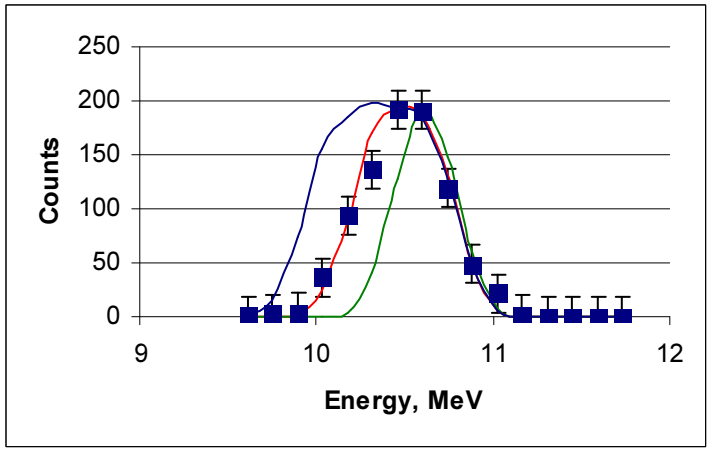

Fig. 14. The experimental energy distribution of tritons (measurement #527) and Monte-Carlo simulation for three different thicknesses of tritium location: 20 (green), 25 (red), 30 (blue) microns. Points with error bars are experimental values.

One can see from these figures that the ratio of the areas of peaks corresponding to tritons and deuterons is 1.0:0.09. Using the known scattering cross sections for neutrons on tritium and deuterium averaged on the aperture of the detector (0 - 7.5°) and equal to 370 and 450 mb/sr respectively, we can conclude that the deuterium concentration relative to tritium in titanium is 0.07, i.e. TiT_2 and $TiD_{0.14}$.

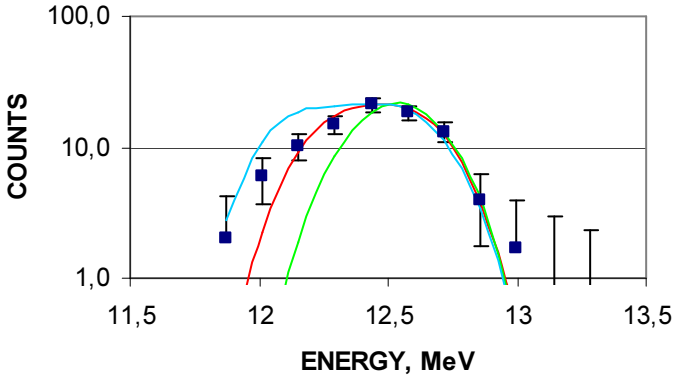

Fig. 15. The experimental energy distribution of deuterons (measurement #527) and the Monte-Carlo simulation for three different thicknesses of deuterium: 25 (green), 35 (red) and 45 (blue) mkm. The best fit is achieved when the tritium thickness is 25 microns.

Summary

- on the basis of the analysis of nuclear interactions of neutrons with nuclei of different constructional materials, a new design has been made of the inner element of the NERD reaction chamber;
- optimization of geometry of measurement was carried out using a program of mathematical simulation based on the Monte-Carlo method;
- topography of the energy resolution corresponding to count rate as a function of base geometrical parameters was obtained;
- rapidity of the electronics was increased;
- basic characteristics of the NERD-spectrometer (depth of analysis, and value of the depth resolution) were improved.

We are planning to do the following:

i. design, manufacture and mount the device for the adjustable translocation of a deuteron beam spot on a target to allow a check of the location of a beam spot;
ii. continue development of the target unit for operation with neutron flux at the optimal angle;
iii. improve the fast gates for decrease of the effect of driving signal on the spectrometric signal;
iv. implement the analysis of the interfering reactions with the triton escape on the nuclei of materials used for thermonuclear reactors;
v. measure the content and the depth profiles of hydrogen isotopes in materials of the thermonuclear reactors.

References

1. G.A. Radyuk, S.V. Artemov, A.A. Karakhodzhaev, V.P. Yakushev, E.A. Zaparov, Ya.S. Abdullaeva, “Modified NERD spectrometer for H-isotopes profiling in various materials” (to be published in Eurasian Nuclear Bulletin).
2. A.P. Tsytovich (1984) “Yadernaya elektronika” Moscow, Energoatomizdat, 1984, pp. 52 (Russian).
3. V.A. Grigor’ev, A.A. Kolyubin, V.A. Loginov (1988) “Elektronnye metody yaderno-fizicheskogo eksperimenta“, Moscow, Energoatomizdat, pp. 137 (Russian).
4. Kh. Shmidt (1989) “Izmeritel’naya elektronika v yadernoy fizike”, Izd. “MIR” Moscow, pp. 72 (Russian).
5. E.A. Kolombet (1991) “Mikroelektronnye sredstva obrabotki analogovykh signalov” Izd. “Radio i svyaz” Moscow, p. 319 (Russian).
6. S.V. Artemov, G.A. Radyuk, V.P. Yakushev, E.A. Zaparov “Using of Monte-Carlo simulation for choice of the parameters of the NERD device”, 5th International Conference “Modern problems of nuclear physics” Samarkand, Uzbekistan, 12-15 August 2003, pp. 129-130.
7. G.A. Radyuk, S.V. Artemov, A.Kh. Abdurakhmanov, V.P. Yakushev, E.A. Zaparov, “Improvement of the neutron-induced elastic recoil detection spectrometer on basis of neutron generator NG-150” Abstract Book of International Conference “NUCLEUS-2004”, Belgorod, (Russia), June 2004, pp. 284.

Use of Tungsten in Future Fusion Reactors

R. Causey

Sandia National Laboratories
Livermore, CA 94550, USA

Tungsten has many properties that make it a serious candidate for fusion reactor applications. It has the highest melting point of all the metals and a relatively high thermal conductivity (~ 45% of that of copper). Still, this material should not retain or permeate large quantities of tritium and should not be released into the plasma if it is to be successfully used in such an application.

A review of the properties controlling the retention and release of hydrogen isotopes from tungsten yield the following parameters: the diffusivity and solubility of hydrogen in tungsten are $D = 4.1 \times 10^{-7} \exp(-0.39\ eV/kT)\ m^2\ s^{-1}$ and $S = 9 \times 10^{-3} \exp(-1.04\ eV/kT)$ H/W $atm^{-1/2}$ [1]. Hydrogen is trapped at vacancies and at dislocations on cell boundaries with an activation energy of approximately 1.4 eV [2, 3]. In the case of voids, there is an additional trap energy of 1.8 to 2.1 eV associated with chemisorption on the walls of the voids [4]. Once tritium has entered tungsten in atomic form, it must undergo recombination into molecules at the surface to be released from the material. The recombination process is given by the formula Release Rate = $K_R C^2$, where K_R is referred to as the recombination rate coefficient. In the case of tungsten, the recombination rate coefficient is effectively infinite [5], yielding C = 0 at the boundary as the correct boundary condition. With the use of the above parameters, and as seen in many experiments, the retention of tritium in tungsten is typically quite small. The use of tungsten in fusion reactors will not result in elevated inventories of tritium.

Blisters generated by the bombardment of tungsten by energetic hydrogen ions are considered by some to be potential problem for the use of tungsten in fusion reactors. In reality, blisters cannot form at higher temperatures, and at lower temperatures, the formation depends on previous cold working and on annealing temperature [6]. For such blisters to form, there must be cold rolling damage that produces planar defects parallel to the surface (rolling direction). In this case, hydrogen isotopes can be trapped at the planar defects, generating stress that pushes the material up from the location of the planar defects. If the rolling was done at higher temperatures, the density of these planar defects is lower. Also, if sufficiently annealed, too few hydrogen atoms are trapped to generate the necessary stress to push up the blister. The bottom line is that blisters do not have to be a problem for fusion applications - they can be prevented.

In conclusion, tungsten should be a candidate material for fusion reactors. The high melting point, high thermal conductivity, low tritium retention characteristics, and resistance to blistering should result in large scale use of tungsten in ITER and future fusion devices.

References

1. R. Frauenfelder, J. Vac. Sci. Technol. 6 (1969) 38.
2. H. Eleveld and A. van Veen, J. Nucl. Mater. 191 (1992) 433.
3. R. Anderl et al., Fus. Technol. 21 (1992) 745.
4. H. Eleveld and A. van Veen, J. Nucl. Mater. 212 (1994) 1421.
5. R. Causey and T. Venhaus, Physica Scripta T94 (2001) 9.
6. T. Venhaus et al., J. Nucl. Mater. 290-293 (2001) 505.

Studies of tritium retention in JET, and de-tritiation

J.P. Coad

UKAEA Fusion Association, Culham Science Centre, Abingdon, OX14 3DB, UK

Programme of Work

Programme of work agreed for UKAEA under the CRP was the following:

1. Analysis of samples removed from the first wall of JET to increase the understanding of where and by what mechanism deposition occurs.
2. Measurement of hydrogen isotope retention during JET operations.
3. Development of techniques for improved temporal resolution of retention and deposition of hydrogen isotopes in JET.
4. Study of methods for in-vessel tritium inventory reduction.
5. Development of de-tritiation techniques for components removed from fusion devices.

Progress in period 2001-2004

1. Analysis of samples removed from the first wall of JET to increase the understanding of where and by what mechanism deposition occurs

A poloidal set of special divertor tiles that were mounted in the JET machine in 1999 has been analysed. These tiles had been accurately measured mechanically, and coated with stripes of C + 10%B on a Re interlayer in order to aid assessment of erosion or deposition. A poloidal set of standard divertor tiles exposed 1998-2001 have also been studied. Deposits up to 100 μm thick have been found generally over the inner divertor, whilst on average little or no erosion/deposition was measurable at the outer divertor. However, dusty deposits up to 200 μm thick were found at the target area for plasma in the extreme inner divertor corner.

The deposited films on the inner divertor wall tiles were duplex in nature. The inner film (~ $^2/_3$ the overall film thickness) was very rich in Be (Be/C ~ 1), similar to the film on tiles removed in 1999 and 1998. However, the outer ~ $^1/_3$ of the film was less enriched in Be (Be/C ~ 0.1), and had a higher D content. It is believed that the change in film composition corresponded to a reduction in the vessel (and thus divertor tile) temperature from 593K to 473K during the latter part of the 1999-2001 operations.

During the last few pulses before the 2001 shutdown, ^{13}C was introduced into the JET vessel, by puffing in $^{13}CH_4$ at the top of the vessel. A total of 1.3 x 10^{23} atom of ^{13}C were introduced. The ^{13}C is clearly seen in a sub-micron layer on the surface of the inner divertor wall tiles, but is not seen at the outer divetrtot, or on the divertor base tiles. The distributions of ^{13}C found, together with the absolute amounts, demonstrate the strong flows of impurities from outboard to inboard in JET, and provide a clear data-set for modelling of the SOL.

Special tiles and samples mounted in other parts of the vessel such as the inner wall and poloidal limiters during the period 1999-2001 have also been analysed to establish the sources for the material deposited at the inner divertor. The outer poloidal limiters are clearly a net erosion area – indeed on parts of some tiles the markers completely disappeared so that only a lower limit for the amount eroded could be determined. The inner protection tiles are also an erosion zone, but again the markers disappeared. The inner guard limiters showed some erosion, but also areas of heavy deposition.

During the present 2004 JET shutdown further sets of divertor and wall tiles are being removed, and another ^{13}C puffing experiment was carried out immediately prior to the shutdown, this time puffing from the outer divertor. Analysis of these tiles over the next two years will provide further information on erosion and deposition processes in JET. For quantitative measurements of erosion and deposition, accurately measured tiles with marker stripes are being installed at many points around the poloidal cross-section of JET during 2004. However, these tiles will not be removed for analysis until a future major JET shutdown, which may not be until 2008.

2. Measurement of hydrogen isotope retention during JET operations

The amount of deuterium retention has been assessed from the analysis of tiles removed in 2001, and shows a somewhat lower retention rate than during DTE1 in 1997. Attempts were made during the last campaign to measure the H isotope retention by gas balance and/or pressure measurements. However, these measurements have a large intrinsic error due to the need to properly account for the in-vessel cryo-pump and pumping through the Neutral Beam ports, and statistics were poor.

In 2003 a trace tritium experiment (TTE) was carried out on JET. 380 mg of tritium were introduced into the torus during a campaign of ~500 pulses. Tritium accountancy over the period showed the same amount of tritium was returned to the gas handling plant. Possibly tritium retained by co-deposition etc during this campaign was off-set by release of T from the reservoir remaining since the DTE1 experiment.

3. Development of techniques for improved temporal resolution of retention and deposition of hydrogen isotopes in JET

A prototype Quartz Micro-Balance (QMB) was installed in JET in 2001 and worked successfully for 2 years, although it was eventually damaged when exposed to a high power flux. Details of the QMB, and results obtained in the period 2001-2004 have been published [1, 2].

Over the past two years new QMBs based on the prototype unit have been designed and built and are ready for installation in JET during the 2004 shutdown. These units are as follows (see Fig. 1):

(i) A replacement in front of the louvres at the inner divertor corner for the prototype unit, which retains the original design.
(ii) A unit in a similar position, but in contact with the water-cooled divertor support structure. This will limit the crystal temperature, by conduction through the mounting system to the support structure. We will then check whether the crystal of the prototype unit was already getting hot enough to limit the sticking coefficient.
(iii) A unit in a similar position, but with a heater for the deposition crystal. This will allow the temperature variation of the sticking coefficient to be explored.
(iv) A unit similar to (iii), but in front of the outer louvres.
(v) A QMB in the septum replacement support structure, viewing radially inwards towards the inner strike point.
(vi) A QMB in the outer divertor carrier looking up at the beryllium evaporator near the outer mid-plane at the same toroidal location. H-isotope retention in the period 1998-2004 relies on the amount of Be deposited at the inner divertor to establish the amount of films deposited. However, this figure cannot be correlated with the

amount of Be evaporation, as no measurements are made of this quantity. This QMB will allow the amount of Be evaporated to be calibrated.

All the QMBs in (i) to (iv) are fitted with shutters so that plasma pulses (or parts thereof) can be selected for measurement.

Rotating collectors have also been designed that rotate under the action of the magnetic field. The collector plate is exposed through a slit, and will rotate during the first 3200 discharges, and any point on the collector will be exposed to 25 – 50 pulses (depending on the slit width). Since there are no electrical connections required, these units can be fitted anywhere in the torus protected from direct interaction with plasma ions. They will be fitted in the divertor and on the wall at the outer mid-plane. However, the data can only be evaluated after the units are removed at a future intervention.

4. Study of methods for in-vessel tritium inventory reduction

During the period of this contract, photon cleaning has been used to de-tritiate tiles *in-situ* in JET. Photon cleaning involves focussing intense UV and visible light from a flash-lamp using a parabolic reflector onto a line on the sample surface. Thus, an area may be treated by sweeping this line across a surface. A 500 J, 5 Hz lamp was mounted in a special housing that could be carried by the MASCOT robotic arm and positioned remotely in JET. Tiles of the inner divertor were treated in JET at high power, so that the deposited film was clearly seen to have been ablated from the surface [3]. A number of Outer Poloidal Limiter (OPL) tiles were then to have been treated at lower power, so that surface films would be out-gassed, but ablation would not occur. However, a problem developed with the lamp, so the treatment was carried out in the Beryllium Handling Facility at JET.

The divertor tiles and OPL tiles that have been treated will now be analysed for tritium and deuterium content and compared with similar tiles that have not been treated, to measure the efficacy of the photon cleaning process.

5. Development of de-tritiation techniques for components removed from fusion devices

Large numbers of carbon tiles that have been used in previous operational campaigns of JET are in store. These tiles are radioactive and Be-contaminated. In particular there are ~ 500 tiles, each with a mass of ~ 5 kg and a T activation of 20 - 50 MBq/g remaining from the Deuterium-Tritium Experiment (DTE1) that was performed in JET in 1997. The objective is to reduce the activity of these tiles in a simple manner so that they could be re-classified as Low Level Waste in the U.K. (activity < 12 kBq/g).

A promising technique that has been evaluated during this period is use of an oxy-gas burner. The oxy-gas burner is a bank of gas jets operating in air (within a glove-box) that heats an area of ~ 200 x 50 mm. By sweeping across a divertor tile, the whole tile could be heated to ~ 1000K in ~ 500 s. Tritium analyses were performed by FZK, Karlsruhe, and the burner trials were carried out at PPPL, Princeton. For the whole tile, a decontamination factor (DF) of 850 was achieved, bringing the activity down to 50 kBq/g. Several smaller pieces of tile were also treated, varying the burner conditions such as number of runs and final temperature, and one piece reached a final activity of 9.6 kBq/g (DF = 2500). Although the technique removes > 99.8% of the tritium, the LLW threshold was not regularly achieved. Surface films containing

the majority of the tritium appear to be effectively removed, whereas tritium within the bulk of the tile is re-distributed but not removed.

6. Conclusions

Considerable effort has been devoted to each of the programme areas during the reporting period, and significant progress has been made.

During 2004 many more plasma-facing components have been removed from JET for analysis, and over the next two years these will provide further information on erosion and deposition mechanisms and the H-isotope retention.

The in-situ photon cleaning by ablation of thick films in a tokamak has been demonstrated, and rates of cleaning are applicable to a large fusion device. Tiles will be analysed over the next year to measure the de-tritiation factors achieved. Further development of the process will continue, to establish the nature of the ablated material (e.g. whether gaseous or some as particulates) and whether the size of the cleaning head can be reduced to allow access to restricted areas.

There are many forms of waste created whilst operating a fusion device, from house-keeping to highly-activated in-vessel components. Further research will be conducted on de-tritiation of these various waste streams.

References

1. H.-G. Esser, G. Neill, J.P. Coad et al., Fusion Eng. Design **66-68** (2003) 855.
2. H.-G. Esser, V. Philipps, M. Freisinger et al., 14th Plasma Surface Interactions Conf., Portland, USA, May 2004 (to be published in J. Nucl. Mat.).
3. G.F. Counsell et al., ibid.

Progress Report

R.P. Doerner

Center for Energy Research, University of California - San Diego, USA

In 2002, collaboration was established between the USDOE and EFDA focusing on the plasma materials interaction behavior of C/Be/W mixed materials. The experimental plan consisted of a systematic series of experimental exposures of carbon and tungsten samples to deuterium plasma seeded with a controllable amount of beryllium impurity ions. These experiments were conducted in the PISCES-B beryllium facility at UCSD. Sample analysis of the targets and witness plate coupons collected during the exposures was carried out predominantly at the IPP in Garching. Modeling of the experiments and their resultant surfaces were undertaken both within the US and EU plasma facing component communities.

The PISCES-B device has been modified in two ways to accomplish this experimental program. First, in order to seed a controllable amount of beryllium impurities into the plasma column a commercial high-temperature effusion cell from Veeco Applied EPI has been installed on PISCES-B. The orientation of the atom beam emerging from this oven is oriented in such a way that the beam travels perpendicular to the magnetic axis of PISCES-B. Due to the rather slow thermal velocity of the Be atoms, some amount of the beam of atoms is attenuated in the plasma column due to ionization. The beryllium ions are then entrained in the plasma flow toward the target. The concentration of beryllium ions within the plasma column is measured by observing the BeII line emission at 467 nm and can be controlled by varying the temperature of the oven. Ionization and excitation rate coefficients were obtained from the ADAS data base. The beryllium ionization rates have previously been experimentally verified in PISCES-B.

The second modification to PISCES-B involved the installation of a movable witness plate manipulator system to collect redeposited material outside of the plasma column during the sample exposures. The samples used to collect material can be either cooled of heated, so that any dependence of the hydrogen inventory in the redeposited mixed materials on the temperature of the plate during deposition can be determined. The witness plate manipulator system was supplied to PISCES-B by the IPP at Garching.

In ITER, the beryllium impurity concentration in the divertor plasma is expected to be in the 1-10% range. We find that even a very small beryllium impurity concentration (as low as 0.2%) is sufficient to dramatically reduce the graphite target chemical and physical erosion rates. Fig. 1a shows the spectroscopic signature of chemical erosion (CD band emission) from a sample exposed at 200°C while Fig. 1b shows the physical sputtering signature (CI line radiation) from a sample exposed at 700°C to deuterium plasma. Data is presented for cases with and without beryllium seeding of the plasma. Weight loss measurements confirm the spectroscopic signature data and indicate a reduction of the total erosion from the graphite samples by more than an order of magnitude when the beryllium concentration in the plasma is as low as 0.2%.

The cause of the reduction becomes apparent during post-exposure surface analysis of the graphite targets. Auger electron spectroscopy of the sample surface exposed at 200°C reveals essentially complete (> 90%) coverage of the graphite sample by a thin beryllium layer as long as the Be seeding concentration exceeds 0.1%. Similar effects are observed during exposure of graphite samples at 1000°C, although a slightly higher Be seeding rate (> 0.3%) is needed to achieve 90% Be surface coverage. This is due to the larger rate of diffusion of Be

into the bulk at the higher temperature, as well as an increase in the Be erosion rate at higher temperature.

The formation of beryllium rich surface layers on the graphite targets also affects the redeposited material collected on the witness plate samples. Fig. 2 shows the elemental depth profile (obtained using x-ray photo-electron spectroscopy (XPS)) of the re-deposited material collected on a tantalum witness plate during exposure of a graphite sample at 700°C to a 0.1% Be seeding rate plasma. The redeposited material is seen to consist almost entirely of beryllium, with only trace amounts of oxygen and carbon throughout most of the layer. The average deuterium content in this layer is consistent with previous retention measurements in 'clean' redeposited beryllium at low temperature as seen in Fig. 3.

While the hydrogen content of beryllium and carbon co-deposited films is found to be similar during room temperature deposition, the hydrogen content in Be films decreases much faster with increasing deposition temperature than that in carbon films. The temperature dependent release of the deuterium from co-deposited material collected during Be seeding experiments is shown in Fig. 4. This data is generated from thermal desorption of the witness plate samples from PISCES-B and can be considered typical of the release behavior of the accumulated co-deposited material in the ITER divertor during a baking cycle. One can see that during a 400°C bake of the ITER divertor (a temperature that is achievable in the ITER divertor after draining of the coolant channels) the D/Be ratio drops to less than 1%. Also shown in the figure for comparison is the temperature dependent deuterium release from co-deposited carbon films.

It is interesting to note that the initial temperature of the wall during the deposition of the material affects the release behavior. The deuterium trapped during room temperature collection is released at lower temperature than that collected during higher temperature wall operation. This may be due to the fact that the material structure will vary depending on the deposition temperature, or it may be related to the oxygen content of the films (see Fig. 3). Work is continuing in this area to try to isolate the cause of the differences.

Another difference between a beryllium-rich and a carbon-rich co-deposit will be in their location. Beryllium has a high sticking coefficient and will be deposited in locations with line-of-sight views of the erosion location, whereas carbon has been found to migrate into pump ducts, behind tiles and to other non-line-of-sight locations.

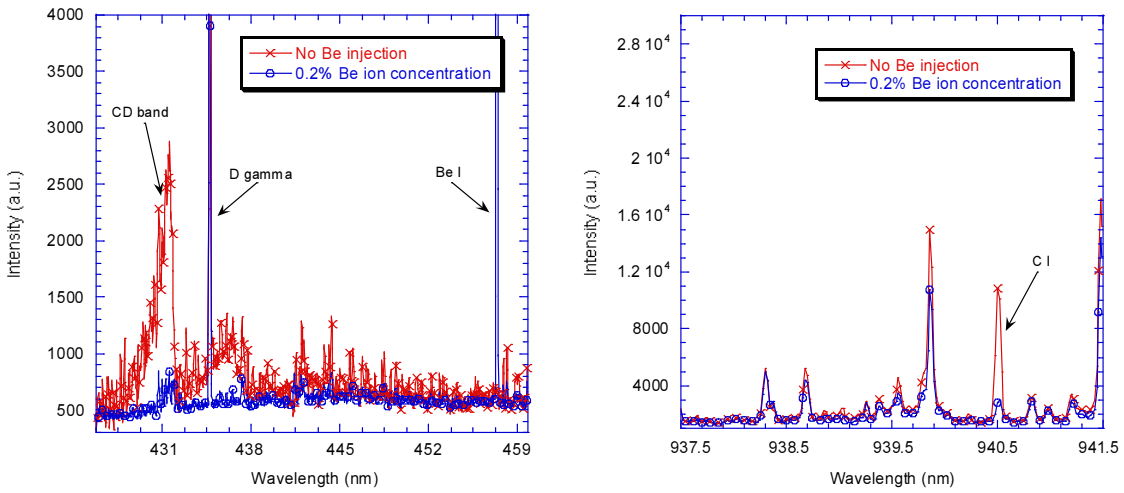

Fig. 1. Beryllium impurity seeding of the incident deuterium plasma reduces both (a) chemical erosion, and (b) physical sputtering of graphite target plates.

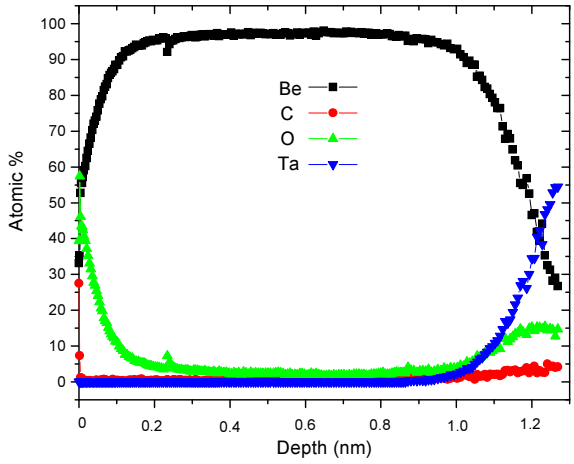

Fig. 2. Depth profile of the composition of a tantalum witness plate sample used to collect re-deposited material during exposure of a 700°C graphite sample to beryllium containing, deuterium plasma.

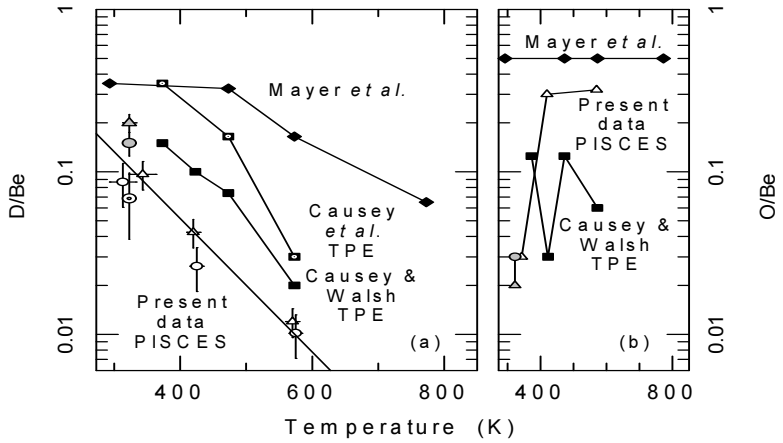

Fig. 3. Deuterium retention in witness plate samples collected during Be seeded plasma exposures.

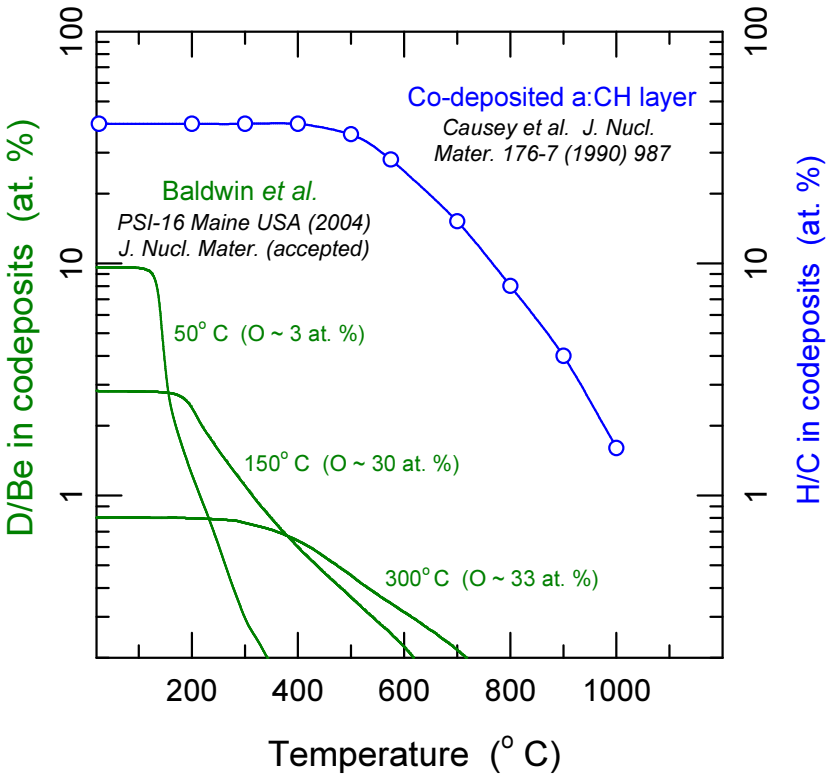

Fig. 4. Thermal release behavior of co-deposited Be films compared with co-deposited carbon films.

References

1. R.P. Doerner et al., Physica Scripta T111 (2004) 75.
2. K. Schmid et al., Nucl. Fusion 44 (2004) 815.
3. M.J. Baldwin et al., J. Nucl. Mater., in press, 2004 (presented at PSI-16).
4. K. Schmid et al., J. Nucl. Mater., in press, 2004 (presented at PSI-16).

Research Progress on Tasks Identified at the 2002 CRP Meeting

A. Haasz

University of Toronto, Canada

Identify Sources and Sinks in Tokamak:

A tokamak probe, the porous plug injection system, has been designed and constructed with the objective of calibrating spectroscopic measurements of chemical erosion in a tokamak divertor. The probe operates by providing a realistically distributed influx of hydrocarbon gas into the divertor which is then monitored through spectroscopic measurements of the dissociation fragments, e.g., CD. Preliminary testing in the DIII-D tokamak has successfully demonstrated the operation of the probe. The first experiment in DIII-D was conducted on 22 October.

Hydrocarbon Species Generation with Tritium: *(task has been completed)*

Experiments on the chemical erosion of carbon due to low energy tritium ion irradiation were performed at the University of Toronto. These were **the first measurements** of chemical erosion yields of graphite by mass-analyzed tritium ions. The distribution of hydrocarbons was also obtained. The results were presented at the 16th PSI Conference in Portland, Maine, in May 2004.

The results show that the chemical erosion yields of graphite for H^+, D^+, and T^+ are very similar in magnitude and temperature dependence. Given the observed absence of a significant isotopic effect for H^+ and D^+ in the 10-200 eV energy range [Mech et al., JNM 1998], and the observed similar yields for H^+, D^+, and T^+ at 200-250 eV [new T^+ results], it is reasonable to assume that no significant isotopic effect is expected for T^+ at energies of tens of eV. Consequently, the chemical erosion rates for H and D provide reasonable estimates of carbon erosion due to T in a fusion reactor.

Effect of Metals on Thermo-Oxidation: *(task will continue)*

We have performed extensive experiments on thermo-oxidation of tokamak codeposits and laboratory-produced films as a function of specimen temperature and oxygen pressure. A key finding was the large variation in codeposit/film erosion rates for the various specimens. It is evident that the codeposit structure has an effect on the erosion rate, but it is also likely that metallic impurities originating from tokamak materials play a role. Controlled experiments were performed with laboratory films onto which we have sputter-deposited sub-monolayers of tungsten. It was anticipated that a catalytic effect might enhance the erosion rate. This, however, was not observed. Further controlled experiments will be performed with specimens having C and W simultaneously sputter-codeposited on the surface; these specimens will be provided by IPP-Garching (J. Roth). Future work will also involve tokamak codeposits with well characterized structure and impurity content.

Retention Measurements with Sprayed Tungsten: *(task has not commenced)*

This task will commence after receipt of sprayed W material from G. Federici.

Effect of O, C Layers on W on H Retention: *(task will continue)*

We have completed experiments on D retention in W after sequential irradiation by C^+ first and then by D^+. The retained D was measured by thermal desorption spectroscopy. The amount of D retained depends on the energy and amount of C^+ implanted. For a relatively thick C layer, the retained D is very similar to the case of D retained in graphite. Upon gradual removal of the C layer by the subsequent D^+ irradiation, the retained amount of D goes from pure graphite to some interface carbide material and then to pure tungsten. Future work will involve D retention measurements for simultaneous C^+ and D^+ irradiation, where the dynamic of having two impacting species present is expected to affect the mixing and retention behaviour.

Additional Activities Related to CRP:

We have commenced retention experiments with W irradiated with D^+ and He^+ ions both sequentially and simultaneously. Deuterium and helium retention is measured by post-irradiation thermal desorption spectroscopy. Initial results are now available.

Progress Report

A. Pisarev

Moscow Engineering and Physics Institute, Russia

Preliminary test experiments on laser induced desorption have been performed using samples from TEXTOR bumper limiter and a pulsed excimer laser. The work was performed in collaboration between the Royal Institute of Technology, Stockholm, Moscow Engineering and Physics Institute, Moscow, and Institute for Plasma Physics, Julich. The samples were taken from the regions of preferential erosion of the TEXTOR limiter, their surface had a flaked structure, which was created by incident plasma impact, and the upper layers contained a thin metal deposits, oxygen and deuterium. Thermal desorption experiments demonstrated that deuterium is released in the low temperature range, which is more typical for metals but not carbon film. Laser irradiations were performed at low power density below ablation threshold and demonstrated high desorption efficiency. One can suggest pulsed lasers could be effective for de-tritiation of metal films, which could be typical depositions in ITER. Further studies are planned.

Hydrogen accumulation and desorption from graphite samples and crystalline boron carbide have been investigated for the case of hydrogen implantation at the energies of 100 eV and 1 keV from gas discharge plasma. The work was performed in collaboration between Moscow Engineering and Physics Institute and University of Nagoya. Experiments were performed at high ion fluences up to 10^{25} H m^{-2}. Thermal de-sorption spectra after implantation were used for measurement of hydrogen retention, and release of H_2 and CH_4 was monitored. It was observed that accumulation of hydrogen in graphite continues at these very high fluences above the fluence necessary for the saturation of the ion range region. It was concluded that accumulation of hydrogen in graphite takes place mainly in the material bulk. It was suggested that deep hydrogen transport is induced by implantation damage (possibly by tensions or radiation vacancies). Not much difference was found in accumulation in a fine grain graphite and CFC. Trapping efficiency in the crystalline B_4C was relatively smaller and tends to zero at high fluences. It was concluded that transport in the B_4C bulk is slow. Release of H_2 and CH_4 were compared. It was found that four peaks (or groups of peaks) 500, 800, 1000 and 1200K are typical for H_2 and one peak at about 800K is typical for CH_4. The net amount of methane is an order of magnitude less. Difference in trapping and release at 100 eV and 1 keV implantation was analysed. No saturation of trapping at the highest fluence was observed at 1 keV. Low temperature peaks dominate in thermal desorption spectra at 100 eV, while high temperature peaks release about 50% of hydrogen trapped at 1 keV. It was concluded that hydrogen is trapped mainly in the destroyed regions not very far from the surface at low ion energy while at the higher energy a lot of hydrogen is trapped in very deep layer with the structure close to the original crystalline structure. Experiments on TDS measurements after removal of a thin (250 Å) layer performed by 100 eV Ar^+ etching also agree with his suggestion: low temperature peaks decrease by etching after 100eV hydrogen implantation, while relatively uniform decrease of all peaks was observed by etching after 1 keV implantation. Hydrogen desorption from graphite being kept in air was investigated. It was surprisingly observed that high temperature peaks decrease first, which has never been observed for metals. It was suggested that the release during keeping in air starts from deep layers and is stimulated by the energy released due to re-crystallisation of damaged upper layers, which in turn is stimulated by undamaged deep layers, which provoke rearrangement of atoms in the “amorphous like” layer in the way they are built up to the underlying crystalline structure. Experiments are planned to verify the results obtained.

Investigation of de-tritiation of oxidized steel in wet Ar has been performed. The work was performed in collaboration between Moscow Engineering and Physics Institute, Russia and the University of Toyama, Japan. The samples of SS316 with heavy technological oxides were saturated in tritium and hold in wet Ar. The tritium retained was measured as a function of time. Computer modeling of retention demonstrated that the experiment is well described by diffusion with subsequent desorption of heavy water. The diffusion coefficients obtained at various temperatures are in a very good agreement with literature data obtained in experiments with clean surfaces. The model suggesting desorption of tritium gas gave formally a good description but wrong values of the diffusivity and desorption coefficient. Thus, it was demonstrated that the limiting process of tritium release in wet atmosphere is diffusion, that T-HO recombination on the surface is very fast, and the thick oxide layer on the surface does not retard release of HTO, probably due to cracks in the oxide. Tritium release from as-received SS in wet atmosphere can even be well described by diffusion with zero boundary conditions.

Summary of research performed

C.H. Skinner

Princeton Plasma Physics Laboratory, USA

Comparison of the thermal response of tungsten pre-blistered by ion bombardment to unblistered tungsten

Tungsten PFCs are planned for ITER divertor baffle and are a candidate for the high heat flux areas of the divertor because tungsten avoids the tritium retention issue. However, the surface of tungsten experiences blistering of the surface under some conditions of high ion bombardment. The blister caps are in reduced thermal contact to the bulk and may experience flaking, melting and evaporation under high heat loads in next step devices. Generation of tungsten dust is a safety issue in next step devices as it is radiologically activated and could be dispersed in accident conditions.

We received tungsten samples, blistered as a result of high fluence D ion flux (courtesy of J. Roth, Max Plank Institute fur Plasmaphysik, Garching) and subjected them to high heat flux from a scanning continuous wave Nd laser. The surface was imaged before and during laser exposure (Fig. 1). Images taken during the laser heating showed hot spots at the location of the blisters. It is clear that blister caps will experience a much higher temperature excursion than an unblistered surface.

(a)  (b) 

Fig. 1. (a) W sample implanted with 10^{21} D @ 200 eV, and (b) during laser irradiation.

Measure temperature rise and morphological changes of graphite and CFC samples during exposure to high heat flux.

The thermo-mechanical response of graphite and carbon fiber composite (CFC) to ELMs disruptions and VDEs includes sublimation, heating and explosion of gases trapped in the pores, and thermal stresses and fatigue. A scanning Nd laser was used to deliver pulses of high heat flux at pulse lengths from 1 to 200 ms. A key result was that the thermal response of tokamak generated codeposits showed striking differences to the manufactured material. The results were published in refs. [1, 2].

Deposition and dust in NSTX

Time-resolved measurements of deposition in current tokamaks are crucial to gain a predictive understanding of deposition with a view to mitigating tritium retention and deposition on diagnostic mirrors expected in next-step devices. Two quartz crystal microbalances have been installed on NSTX at a location 0.77 m outside the last closed flux

surface. This configuration mimics a typical diagnostic window or mirror. The deposits were analyzed *ex-situ* and found to be dominantly carbon, oxygen and deuterium. A rear facing quartz crystal recorded deposition of lower sticking probability molecules at 10% of the rate of the front facing one. Time resolved measurements over a 4-week period with 497 discharges, recorded 29.2 $\mu g/cm^2$ of deposition, however surprisingly, 15.9 $\mu g/cm^2$ of material loss occurred at 7 discharges. The net deposited mass of 13.3 $\mu g/cm^2$ matched the mass of 13.5 $\mu g/cm^2$ measured independently by ion beam analysis. Monte Carlo modeling suggests that transient processes are likely to dominate the deposition [3].

In next-step devices the amount of dust generated is likely to scale-up by two or three orders of magnitude as the erosion increases both with the pulse length and the increase in heat flux during ELMs and disruptions. Dust will be radiologically and chemically hazardous and will go from being largely inconsequential, to a major factor in safety assessments, site licensing, and tokamak operations. Dust particles that had accumulated on a viewport the bottom of the NSTX vessel at bay B during the period 20 January – 5 March 2004 (520 discharges) were examined with a digital optical microscope. The viewport views the plasma through a 5 cm wide slot on the inner lower passive plate and is 40 cm below the ATJ graphite tiles. The particle density was measured to be 313 500 particles/cm^2 with the most common size being 1μm. Raman analysis showed the particles to be disordered graphitic (sp^2) carbon, easily recognized by the presence of the typical D-band ~ 1330 cm^{-1} and G-band at 1585 cm^{-1}. The first results from a novel electrostatic dust detector were presented [4].

References

1. C. H. Skinner, N. Bekris, J. P. Coad, C. A. Gentile and M. Glugla. Tritium Removal from JET and TFTR Tiles by a scanning laser, J. Nucl. Mater. 313-316 (2003) 496-500.
2. C. H. Skinner, N. Bekris, J. P. Coad, C. A. Gentile, A. Hassanein, R. Reiswig and S. Willms. Thermal Response of Tritiated Co-deposits from JET and TFTR to transient heat pulses, Physica Scripta T103 (2003) 34-37.
3. C. H. Skinner, H. Kugel, J Hogan W. Wampler and the NSTX team. Time resolved hydrocarbon deposition in NSTX, 16th International Conference on Plasma Surface Interactions, Portland, Maine, USA, 24-28 May 2004, to be published in J. Nucl. Mater. (2005).
4. C. H. Skinner, A. L. Roquemore, A. Bader, W. R. Wampler and the NSTX team. Deposition diagnostics for next-step devices, Rev. Sci. Instrum. **75** (2004).

Nuclear Data Section
International Atomic Energy Agency
P.O. Box 100
A-1400 Vienna
Austria

e-mail: services@iaeand.iaea.org
fax: (43-1)26007
cable: INATOM VIENNA
telex: 1-12645
telephone: (43-1)2600-21710